IEEE Guide for the Measurement of DC Electric-Field Strength and Ion Related Quantities

American National Standards Institute
Approved October 12, 1990

IEEE Standards Board
Approved May 31, 1990

Sponsor
Transmission and Distribution Committee
of the
IEEE Power Engineering Society

Abstract: IEEE Std 1227-1990, IEEE Guide for the Measurement of DC Electric-Field Strength and Ion Related Quantities (ANSI), provides guidance for measuring the electric-field strength, ion-current density, conductivity, monopolar space-charge density, and net space-charge density in the vicinity of HVDC power lines, in converter substations, and in apparatus designed to simulate the HVDC power-line environment.

Keywords: conductivity, electric-field strength, ion-current density, monopolar space-charge density, net space-charge density, power lines.

Library of Congress Catalog Number: 90-056232

ISBN 1-55937-073-4

Copyright 1990 by **The Institute of Electrical and Electronics Engineers, Inc. 345 East 47th Street, New York, NY 10017-2394, USA**

No part of this publication may be reproduced in any form, in an electronic retrieval system or otherwise, without the prior written permission of the publisher.

IEEE Standards documents are developed within the Technical Committees of the IEEE Societies and the Standards Coordinating Committees of the IEEE Standards Board. Members of the committees serve voluntarily and without compensation. They are not necessarily members of the Institute. The standards developed within IEEE represent a consensus of the broad expertise on the subject within the Institute as well as those activities outside of IEEE which have expressed an interest in participating in the development of the standard.

Use of an IEEE Standard is wholly voluntary. The existence of an IEEE Standard does not imply that there are no other ways to produce, test, measure, purchase, market, or provide other goods and services related to the scope of the IEEE Standard. Furthermore, the viewpoint expressed at the time a standard is approved and issued is subject to change brought about through developments in the state of the art and comments received from users of the standard. Every IEEE Standard is subjected to review at least every five years for revision or reaffirmation. When a document is more than five years old and has not been reaffirmed, it is reasonable to conclude that its contents, although still of some value, do not wholly reflect the present state of the art. Users are cautioned to check to determine that they have the latest edition of any IEEE Standard.

Comments for revision of IEEE Standards are welcome from any interested party, regardless of membership affiliation with IEEE. Suggestions for changes in documents should be in the form of a proposed change of text, together with appropriate supporting comments.

Interpretations: Occasionally questions may arise regarding the meaning of portions of standards as they relate to specific applications. When the need for interpretations is brought to the attention of IEEE, the Institute will initiate action to prepare appropriate responses. Since IEEE Standards represent a consensus of all concerned interests, it is important to ensure that any interpretation has also received the concurrence of a balance of interests. For this reason IEEE and the members of its technical committees are not able to provide an instant response to interpretation requests except in those cases where the matter has previously received formal consideration.

Comments on standards and requests for interpretations should be addressed to:

Secretary, IEEE Standards Board
445 Hoes Lane
P.O. Box 1331
Piscataway, NJ 08555-1331
USA

IEEE Standards documents are adopted by the Institute of Electrical and Electronics Engineers without regard to whether their adoption may involve patents on articles, materials, or processes. Such adoption does not assume any liability to any patent owner, nor does it assume any obligation whatever to parties adopting the standards documents.

Contents

Foreword

(This Foreword is not a part of IEEE Std 1227-1990, IEEE Guide for the Measurement of DC Electric-Field Strength and Ion Related Quantities.)

Because of interest in the electrical environment near high-voltage dc transmissions lines, the DC Fields and Ions Working Group felt that there was a need to prepare a document that would provide some guidance for the measurement of several relevant electrical parameters. The electrical parameters that are considered in this standard include the electric-field strength, the ion-current density, the monopolar charge density, and the net space-charge density.

The working group expresses its appreciation to Martin Misakian for his work in preparing the draft of this document in collaboration with members of the working group. The text of the standard includes the results of many studies by researchers at the Bonneville Power Administration, the Electric Power Research Institute's High-Voltage Transmission Research Center, Institut de Recherche d'Hydro-Québec, the Jet Propulsion Laboratory, and the National Institute of Standards and Technology. These studies were supported by internal funding, as well as by funding from the U.S. Department of Energy and the Electric Power Research Institute. Constructive suggestions from those committees that had requested coordination have also been incorporated into the text.

At the time this standard was completed, the DC Field and Ions Working Group had the following membership:

G. B. Johnson, ***Chair***

R. S. Banks	R. E. Harrison	M. Poland
G. K. Bell	W. Janischewskyj	M. A. Reavis
D. W. Boys	H. Kirkham	S. A. Sebo
T. D. Bracken	P. S. Maruvada	M. Silva
V. L. Chartier	T. J. McDermott	G. Skarbakka
C. C. Diemond	M. Misakian	R. D. Stearns
F. M. Dietrich	P. D. Pedrow	Y. Sunaga
G. Gela		R. Weigel

The following persons were on the balloting committee that approved this document for submission to the IEEE Standards Board:

J. J. Burke	G. Karady	T. J. McDermott
V. L. Chartier	N. Kolcio	F. D. Myers
C. C. Diemond	C. P. Krishnayya	D. L. Nickel
T. Garrity	K. E. Lindsey	S. Nilsson
G. Gela	H. P. Lips	R. G. Oswald
D. A. Gillies	J. H. Mallory	F. S. Prabhakara
I. S. Grant	P. S. Maruvada	W. E. Reid
J. E. Holladay	T. J. McCarthy	F. A. M. Rizk
W. Janischewskyj	T. R. McComb	H. Schneider
J. G. Kappenman		T. Wu

When the IEEE Standards Board approved this standard on May 31, 1990, it had the following membership:

Marco W. Migliaro, ***Chair***
James M. Daly, ***Vice Chair***
Andrew G. Salem, ***Secretary***

Dennis Bodson	Kenneth D. Hendrix	Lawrence V. McCall
Paul L. Borrill	John W. Horch	L. Bruce McClung
Fletcher J. Buckley	Joseph L. Koepfinger*	Donald T. Michael*
Allen L. Clapp	Irving Kolodny	Stig Nilsson
Stephen R. Dillon	Michael A. Lawler	Roy T. Oishi
Donald C. Fleckenstein	Donald J. Loughry	Gary S. Robinson
Jay Forster*	John E. May, Jr.	Terrance R. Whittemore
Thomas L. Hannan		Donald W. Zipse

*Member Emeritus

IEEE Guide for the Measurement of DC Electric-Field Strength and Ion Related Quantities

1. Purpose

The purpose of this document is to provide guidance for the measurement of the electric-field strength, ion-current density, conductivity, monopolar space-charge density, and net space-charge density in the vicinity of high-voltage dc (HVDC) power lines, in converter substations, and in apparatus designed to simulate the HVDC power-line environment. The document

- — Defines the terms that are used
- — Describes the interrelationship between electrical parameters
- — Describes operating principles of measuring instruments
- — Suggests methods of calibration where applicable
- — Describes measurement procedures
- — Identifies significant sources of measurement error

2. Definitions

For additional definitions, see IEEE Std 100-1988 [1] and IEEE Std 539 [3].

charged aerosol: Ion comprised of charged particles, liquid or solid, suspended in air. Typical radius is in the range of 2 x 10^{-8} m to 2 x 10^{-7} m. Mobility is in the range of 10^{-9} m to 10^{-7} m^2/Vs.

NOTE—Historically, these have been referred to as large or Langevin ions. The use of the term “charged aerosols” is encouraged.

corona: A luminous discharge due to ionization of the air surrounding an electrode caused by a voltage gradient exceeding a certain critical value.

current density: A vector-point function describing the magnitude and direction of charge flow per unit area. The preferred unit is amperes per square meter (A/m^2).

dc electric-field strength (dc electric field): The time-invariant electric field, produced by dc power systems and space charge, defined by its space components along three orthogonal axes. The magnitudes of the components are expressed in volts per meter (V/m).

NOTES:

1— The convention in the discussion of electric fields near HVDC transmission lines has been to designate the electric field into the ground as positive; i.e., the electric field under a positive conductor is denoted as positive.

2—The "time-invariant" electric field in this definition is an idealization of actual conditions. Typically, climatic effects will perturb the space charge, which will then perturb the electric-field strength.

electric conductivity: The property of a material or medium permitting flow of electricity through its volume, expressed as the ratio of the electric-current density to electric-field strength in a material or medium. For isotropic homogeneous media, the conductivity is a scalar quantity with the preferred unit, siemens per meter (S/m); 1 S/m = 1 mho/m.

Faraday cage: A conducting enclosure that is used to measure the net space charge per unit volume. *Syn:* **space charge cage, space charge density meter.**

field mill: A device in which a conductor is alternately exposed to the electric field to be measured and then shielded from it. *Syn:* **generating voltmeter, generating electric-field meter.**

NOTE—The resulting induced current to the conductor is a measure of the electric-field strength at the conductor surface

form factor: An empirical parameter representing the increased electric field at the surface of a dc field meter that is mounted above the ground plane. The increased field is due to field perturbation by the instrument. In a uniform field, the unperturbed electric field is given by the measured field divided by the form factor for the instrument.

ion: The isolated atom, molecule, molecular cluster, or aerosol that by loss or gain of one or more electrons has acquired a net electric charge.

NOTE—The inclusion of aerosols (particles) under this definition is consistent with historical usage. The use of the terms "small ion" and "charged aerosol" is encouraged.

ion counter: An instrument that determines monopolar space-charge density by measuring the charge collected from a known volume of air.

ion mobility: The drift speed of an ion in a liquid or gas per unit electric-field strength. The preferred unit is m^2/Vs; another commonly used unit is cm^2/Vs.

large ion: See **charged aerosol.**

medium ion: Ion comprised of several molecules or molecular clusters bound together by charge that is larger and less mobile than a small ion due to more mass or a greater number of molecular clusters. Typical radius is in the range of 10^{-9} m to 2 x 10^{-8} m. Mobility is in the range of 10^{-7} m^2/Vs to 10^{-5} m^2/Vs.

monopolar ion density: The number of ions of a given polarity per unit volume. The preferred unit is m^{-3}; another commonly used unit is cm^{-3}.

monopolar space-charge density: The density of space charge of one polarity. The preferred unit is C/m^3.

net space charge: The free unbalanced charge in a given region, taking no account of the charges of both signs that balance each other. The preferred unit is the coulomb (C).

NOTE—The term "space charge" is often used to refer to net space charge.

net space-charge density: Net space charge (space charge) per unit volume. The preferred unit is C/m^3. This

quantity provides no information about the monopolar space-charge density.

small ion: An ion comprised of molecules or molecular clusters bound together by charge. Mobilities are in the range of 10^{-5} m^2/Vs to 2 x 10^{-4} m^2/Vs. Typical radius is less than 1 x 10^{-9} m.

NOTE—To avoid confusion with the more general term "ion," the use of the term "small ion" is encouraged.

space-charge filter: A device used to measure net space-charge density in which a filter medium is used to remove the charge from an air stream.

vibrating probe: A device in which a plate is modulated below an aperture of a face plate in the electric field to be measured. *Syn:* **vibrating plate electric-field meter.**

NOTE—The meter responds to the oscillating displacement current from the induced charge on the vibrating plate by generating a negative feedback voltage on the face plate to null the signal from the vibrating plate. The electric-field strength is proportional to the feedback voltage.

Wilson plate: A conducting plate that is grounded through an ammeter; it is used to collect the ion current, which is measured as it flows through the ammeter. The plate is sensitive to both ion-current density and changes in electric field (displacement current). *Syn:* **current plate; ion-current plate.**

NOTE—Long integration times are used to minimize the effects of the changes in the electric field (displacement current). If the power-line voltage and geometry are constant with time, the average displacement current is zero.

3. Formula Symbols

This section provides a list of symbols used in the formulas that appear in this guide. While the same symbol is sometimes used to designate more than one physical parameter, there should be little confusion because of the very different contexts in which they are used. The use of SI units for all the physical parameters is encouraged.

E	Electric-field strength
J	Ion-current density
K	Average ion mobility
ρ	Monopolar charge density
v_a	Wind velocity
q_s	Induced charge—shutter-type field mill
$\in_0$	Permittivity of free space
$a(t)$	Sensing electrode area—shutter-type field mill
$i(t)$	Induced current—shutter-type field mill
q_c	Induced charge—cylindrical field mill
L	Cylinder length—cylindrical field mill; side dimension of plate of parallel-plate system; distance ion travels in duct; side dimension of cubical Faraday cage
r^0	Cylinder radius—cylindrical field mill
i_c	Induced current—cylindrical field mill
d	Spacing of parallel plates
V	Voltage
v	Volume of electric-field meter probe
D	Distance between center of electric-field meter probe and either plate of a parallel-plate system

$E(z)$	Electric-field strength as function of height above bottom plate of parallel-plate system with space charge
$\phi(z)$	Electric space potential as function of height above bottom plate of parallel-plate system with space charge
V_t	Voltage of top plate of parallel-plate system
E_t	Electric field at top plate of parallel-plate system with space charge
A	Area of Wilson plate
I	Ion current
R	Resistance value; radius of duct
λ	Electrical conductivity of air
M_0	Volumetric flow rate
C	Interelectrode capacitance of Gerdien table
k	Ion mobility; Boltzmann constant
k_c	Critical ion mobility
$f(k)$	Mobility distribution function
$f(k)dk$	Number of ions with mobility between $k$and $k+dk$
e	Charge of electron; charge of ion
N	Number of ions
$\rho(L)$	Charge density after charge traverses distance L in cylindrical duct
ρ_0	Charge density at entrance of duct; monopolar charge density outside hemispherical Faraday cage
u	Air velocity in duct
τ	Ion time-of-flight
s	Radially outward displacement of ions due to Coulomb repulsion
s'	Radially outward displacement of ions due to diffusion
T	Temperature in degrees K
$\phi(x,y,z)$	Space potential in Faraday cage
ρ_s	Net space-charge density
a,b,c	Dimensions of Faraday cage
i,j,k	Odd integers in summation
ϕ	Space potential at center of cubical Faraday cage
ϕ'	Space potential at center of cylindrical Faraday cage
ρ_i	Monopolar charge density inside hemispheric Faraday cage
E_0	Uniform electric-field strength in vicinity of hemispheric Faraday cage

4. References

This guide shall be used in conjunction with the following publications:

[1] IEEE Std 100-1988, IEEE Standard Dictionary of Electrical and Electronics Terms.[1]

[2] IEEE Std 510-1983, IEEE Recommended Practices for Safety in High-Voltage and High-Power Testing.

[1]IEEE publications are available from the Institute of Electrical and Electronics Engineers, Service Center, 445 Hoes Lane, P.O. Box 1331, Piscataway, NJ 08855-1331, USA.

[3] IEEE Std 539, IEEE Standard Definitions of Terms Relating to Corona and Field Effects of Overhead Power Lines.[2]

[4] IEEE Std 644-1987, IEEE Standard Procedures for Measurement of Power Frequency Electric and Magnetic Fields from AC Power Lines.

[5] Anderson, R. V. "Absolute Measurements of Atmospheric Charge Density." *Journal of Geophysical Research*. vol. 71, 1966, pp. 5809–5814.

[6] Asano, K. "Electrostatic Potential and Field in a Cylindrical Tank Containing Charged Liquid." *Proceedings of the IEE*. vol. 124, 1977, pp. 1277–1281.

[7] Bent, R. B. "The Testing of Apparatus for Ground Fair-Weather Space-Charge Measurements." *Journal of Atmospheric and Terrestrial Physics*. vol. 26, 1964, pp. 313–318.

[8] Bracken, T. D. "Electrical Parameters of the High-Voltage Direct-Current Transmission-Line Environment." *Biological Effects of Extremely Low Frequency Electromagnetic Fields* (Proceedings of the Eighteenth Annual Hanford Life Sciences Symposium at Richland, WA). Phillips et al., eds., 1978, pp. 485–500.

[9] Bracken, T. D., Capon A. S., and Montgomery, D. V. "Ground Level Electric Fields and Ion Currents on the Celilo-Sylmar ± 400 kV DC Intertie During Fair Weather." *IEEE Transactions on Power Apparatus and Systems*. vol. PAS-97, March/April 1978, pp. 370–378.

[10] Bracken, T.D. and Furumasu, B.C. "Fields and Ion Current Measurements in Regions of High Charge Density Near Direct Current Transmission Lines." *Proceedings of the Conference on Cloud Physics and Atmospheric Electricity.* Issaquah, Washington, August 1978. Boston: American Meteorological Society, pp. 544–551.

[11] Carter, P. J. and Johnson, G. B. "Space Charge Measurements Downwind From A Monopolar 500 KVDC Transmission Line." *IEEE Transactions on Power Delivery.* vol. 3, 1988, pp. 2056–2063.

[12] Chalmers, J. A. *Atmospheric Electricity,* 2d ed. Oxford: Pergamon Press, 1967, pp. 94–98.

[13] Chalmers, J.A. "The Measurement of the Vertical Electric Current in the Atmosphere." *Journal of Atmospheric and Terrestrial Physics*. vol. 24, 1962, pp. 297–302.

[14] Charry, J.M., Bailey, W.H., Shapiro, M.H., and Weiss, J.M. Ion Exposure Chambers for Small Animals." *Bioelectromagnetics*. vol. 7, 1986, pp. 1–11.

[15] Charry, J.M., Cerniglia, P.A., Weiss, J.M., Finger, R.F., and Michel, T. J. "Inhalation Chambers for Air Ion Research." *Bioelectromagnetics*. vol. 4, 1983, pp. 167–180.

[16] Chartier, V.L., Dickson, L. D., Lee, L. T., and Stearns, R. D. "Performance of A Long-Term Unattended Station for Measuring DC Fields and Air Ions From An Operating HVDC Line." Paper 88 SM 560-5, 1988, IEEE Summer Power Engineering Society Meeting, Portland, OR.

[17] Comber, M.G. and Johnson, G.B. "HVDC Field and Ion Effects Research at Project UHV: Results of Electric Field and Ion Current Measurements." *IEEE Transactions on Power Apparatus and Systems*. vol. PAS-101, 1982, pp. 1998–2006.

[18] Comber, M.G., Kotter, R., and McKnight, R. "Experimental Evaluation of Instruments for Measuring DC Transmission Line Electric Fields and Ion Currents." *IEEE Transactions on Power Apparatus and Systems*. vol. PAS-102, 1983, pp. 3549–3557.

---

[2]This standard will be available from the Institute of Electrical and Electronics Engineers, Service Center, 445 Hoes Lane, P.O. Box 1331, Piscataway, NJ 08855-1331, USA, in early 1991.

[19] Crozier, W. D. “Electrode Effect during Nighttime Low-Wind Periods.” Journal of Geophysical Research. vol. 68, 1963, pp. 3451–3458.

[20] Dallaire, R.D. and Maruvada, P.S. “Corona Performance of a ±450 kV Bipolar DC Transmission Line Configuration.” *IEEE Transactions on Power Delivery.* vol. PWRD-2, 1987, pp. 477–485.

[21] DiPlacido, J., Shih, C.H., and Ware, B.J. “Analysis of the Proximity Effects in Electric Field Measurements.” *IEEE Transactions on Power Apparatus and Systems*. vol. PAS-97, 1978, pp. 2167–2177; Misakian, M. and Kotter, F.R. Discussion, ibid. pp. 2175–2176.

[22] Electrostatic and Electromagnetic Effects Working Group Paper. “Measurement of Electric and Magnetic Fields From Alternating Current Power Lines.” *IEEE Transactions on Power Apparatus and Systems*. vol. PAS-97, 1978, pp. 1104–1114.

[23] EPRI Report EL-2419, “HVDC Transmission Line Research.” Interim Report for Research Project 1282-2, May 1982.

[24] Fry, T.C. “Two Problems In Potential Theory.” *American Mathematical Monthly.* vol. 39, 1932, pp. 199–209.

[25] Gathman, S.G. “Guarded Double Field Meter.” *Review of Scientific Instruments*. vol. 39, 1968, pp. 43–47.

[26] Gathman, S.G. and Trent, E.A. “Absolute Electric Field Measurements Using Field Mills.” NRL Report 6538, Naval Research Laboratory, Washington, D.C., April 1967.

[27] Harnwell, G. P. and Van Voorhis, S. N. “An Electrostatic Generating Voltmeter.” *Review of Scientific Instruments*. vol. 4, 1933, pp. 540–541.

[28] Hendrikson, R. C. “Space Charge Drift From A ± 400 kV Direct Current Transmission Line.” *Bioelectromagnetics*. vol. 7, 1986, pp. 369–379.

[29] Higazi, K.A. and Chalmers, J.A. “Measurements of Atmospheric Electrical Conductivity Near the Ground.” *Journal of Atmospheric and Terrestrial Physics*. vol. 28, 1966, pp. 327–330.

[30] Hill, H. L., Capon, A. S., Ratz, O., Renner, P. E., and Schmidt, W. D. *Transmission Line Reference Book HVDC to ±600 kV.* Palo Alto: Electric Power Research Institute.

[31] Hill, M. L. and Hoppel, W. A. “Effects of Velocity and Other Physical Variables on the Currents and Potentials Generated by Radioactive Collectors in Electric Field Measurements.” *Electrical Processes In Atmospheres*. H. Dolezalek and R. Reiter, eds. Darmstadt: Steinkopff, 1977, pp. 238–248.

[32] Hoppel, W.A. “Measurement of the Mobility Distribution of Tropospheric Ions.” *Pure and Applied Geophysics*. vol. 81, 1970, pp. 230–245.

[33] Hutchison, W.C.A. “Atmospheric Electric Field Charge Compensation When Measuring Air-Earth Conduction and Precipitation Currents.” *Journal of Atmospheric and Terrestrial Physics*. vol. 28, 1966, pp. 823–830.

[34] Israel, H. *Atmospheric Electricity, vols. I and II*. Translated from the German edition; 1971, 1973; p. 131 ff.

[35] Johnson, G.B. “Electric Fields and Ion Currents of a ±400 kV HVDC Test Line.” *IEEE Transactions on Power Apparatus and Systems*. vol. PAS-102, 1983, pp. 2559–2568.

[36] Johnson, G. B. and Zaffanella, L. E. “Techniques for Measurements of the Electrical Environment Created by HVDC Transmission Lines.” *Proceedings of the Fourth International Symposium on High Voltage Engineering*. Athens, Greece, 1983.

[37] Johnston, A. R. and Kirkham, H. “A Miniaturized Space Potential D. C. Electric Field Meter.” *IEEE Transactions on Power Delivery.* vol. 4, no. 2, 1989, pp. 1253–1261.

[38] Johnston, A. R., Kirkham, H., and Eng, B. T. “dc electric field meter with fiber-optic readout.” *Review of Scientific Instruments*. vol. 57, 1986, pp. 2746–2753.

[39] Kasimer, H. W. “The Cylindrical Field Mill.” *Meteorologische Rundschau*. vol. 25, 1972, pp. 33–38.

[40] Kasimer, H.W. and Ruhnke, L.H. “Antenna Problems of Measurement of the Air-Earth Current.” *Recent Advances in Atmospheric Electricity—Proceedings of the Second Conference on Atmospheric Electricity.* Smith, L.G., ed. Portsmouth, N.H.: Pergamon, 1958.

[41] Kaune, W.T., Gillis, M., and Weigel, R.J. “Techniques for Estimating Space-charge Densities in Systems Containing Air Ions.” *Journal of Applied Physics*. vol. 54, 1983, pp. 6267–6273.

[42] Kirkham, H. and Johnston, A. “Magnetic and Electric Field Meters Developed for the U.S. Department of Energy.” Jet Propulsion Laboratory Publication 88-1, January, 1988, Appendix A.

[43] Kirkham, H., Johnston, A., Jackson, S., and Sheu, K. *AC and DC Electric Field Meters Developed for the U. S. Department of Energy, Department of Energy.* Report No. DOE/ET29372-7, Jet Propulsion Laboratory Report No. 87-20, February 1987.

[44] Kirkpatrick, P. and Miyake, I. “A Generating Voltmeter for the Measurement of High Potentials.” *Review of Scientific Instruments*. vol. 3, 1932, pp. 1–8.

[45] Knoll, M., Eichmerer, J., and Schon, R.W. “Properties, Measurements and Bioclimatic Action of “Small” Multimolecular Atmospheric Ions.” *Advances in Electronics and Electron Physics*. vol. 19, 1964, pp. 177–254.

[46] Kotter, F.R. and Misakian, M. “AC Transmission Line Field Measurements.” NBS Report No. HCP/T-6010/E1 (1977).

[47] Kraakevik, J.H. “The Airborne Measurement of Atmospheric Conductivity.” *Journal of Geophysical Research*. vol. 63, 1958, pp. 161–169.

[48] Lehtimaki, M. and Graeffe, G. “Measurement of Air Ions.” *Environment International*. vol. 12, 1986, pp. 109–113.

[49] Maruvada, P. S., Dallaire, R. D., Norris-Elye, O. C., Thio, C. V,. and Goodman, J. S. “Environmental Effects of the Nelson River-HVDC Transmission Lines—RI, AN, Electric Field, Induced Voltage, and Ion Current Distribution Tests.” *IEEE Transactions on Power Apparatus and Systems*. vol. PAS-101, 1982, pp. 951–959.

[50] Maruvada, P.S., Dallaire, R. D., and Pedneault, R. “Development of Field-Mill Instruments for Ground-Level and Above-Ground Electric Field Measurement Under HVDC Transmission Lines.” *IEEE Transactions on Power Apparatus and Systems*. vol. PAS-102, 1983, pp. 738–744.

[51] Maruvada, P.S. and Drogi, S. “Field and Ion Interactions of Hybrid AC/DC Transmission Lines.” Paper 87 WM 155-5, 1987. IEEE Power Engineering Society Winter Meeting.

[52] McKnight, R. H. “Measurement of Electric Fields and Ion Related Quantities.” *Air Ions: Physical and Biological Aspects*. J. M. Charry and R. Kavet, eds. Boca Raton, FL: CRC Press, 1987, pp. 23–69.

[53] McKnight, R. H. “The Measurement of Net Space Charge Density Using Air Filtration Methods.” *IEEE Transactions Power Apparatus and Systems*. vol. PAS-104, 1985, pp. 971–976.

[54] McKnight, R.H., Kotter, F.R., and Misakian, M. “Measurement of Ion Current Density at Ground Level in the Vicinity of High Voltage DC Transmission Lines.” *IEEE Transactions on Power Apparatus and Systems*. vol. PAS-102, 1983, pp. 934–941.

[55] Misakian, M., “Calibration of Flat 60-Hz Electric Field Probes.” *Bioelectromagnetics*. vol. 5, 1984, pp. 447–450.

[56] Misakian, M. “Generation and measurement of dc electric fields with space charge.” *Journal of Applied Physics*. vol. 52, 1981, pp. 3135–3144.

[57] Misakian, M., McKnight, R., and Fenimore, C. “Calibration of Aspirator-Type Ion Counters and Measurement of Unipolar Charge Densities.” NBS Technical Note 1223, 1986.

[58] Misakian, M., McKnight, R., and Fenimore, C. “Calibration of Aspirator-Type Ion Counters and Measurement of Unipolar Charge Densities.” *Journal of Applied Physics*. vol. 61, 1987, pp. 1276–1287.

[59] Morse, P.M. and Feshbach, H. *Methods of Theoretical Physics, Part II*. New York: McGraw Hill, 1953, p. 1245.

[60] Pedrow, P. D. and Wang, Q. Y. “Floating Potential As A Function of Wind Speed and Direction for a Radioactive Potential Probe.” Paper 44.06, Sixth International Symposium on High Voltage Engineering. New Orleans, LA, August 28–September 1, 1989.

[61] Secker, P. E. and Chubb, J. N. “Instrumentation for Electrostatic Measurements.” *Journal of Electrostatics*. vol. 16, 1984, pp. 1–19.

[62] Smiddy, M. and Chalmers, J.A. “The Double Field-mill.” *Journal of Atmospheric and Terrestrial Physics*. vol. 7, 1958, pp. 206–210.

[63] Smith, L.G. “On the Calibration of Conductivity Meters.” *Review of Scientific Instruments*. vol. 24, 1953, p. 998.

[64] Swann, W.F.G. “On Certain Matters Relating to the Theory of Atmospheric-Electric Measurements.” *Terrestrial Magnetism and Atmospheric Electricity.* vol. 19, 1914, pp. 205–218.

[65] Takuma, T., Kawamoto, T., and Sunaga, Y. “Analysis of Calibration Arrangements for AC Field Strength Meters.” *IEEE Transactions on Power Apparatus and Systems*. vol. PAS-104, 1985, pp. 489–496.

[66] Tammet, H.F. *The Aspiration Method for the Determination of Atmospheric-Ion Spectra, Translated from Russian*. 1970, p. 39 ff.

[67] Vonnegut, B. and Moore, C. B. “A Study of Techniques for Measuring the Concentration of Space Charge in the Lower Atmosphere.” Final Report to Air Force Cambridge Research Center, Contract 19 (604) 1920, January 1958.

[68] Vosteen, R. E., “D. C. Electrostatic Voltmeters and Fieldmeters.” *Conference Record of Ninth Annual Meeting of the IEEE Industrial Applications Society.* October 1974.

[69] Ziesse, N. G. and Penney, G. W. “The Effects of Cigarette Smoke on Space Charge Soiling of Walls when Air is Cleaned by a Charging-type Electrostatic Precipitator.” *ASHRAE Transactions*. vol. 74, 1968, pp. 104–113

[70] Ziesse, N. G. and Penney, G. W. “Some Effects of Particle Size on Measurements of Fine Airborne Particulates.” *ASHRAE Transactions*. vol. 76, 1970, pp. 26–36.

5. Electrical Parameters Near HVDC Transmission Lines

The electrical environment in the vicinity of HVDC transmission lines is characterized by several electrical parameters including the electric-field strength ($\vec{E}$), the ion-current density ($\vec{J}$), and the monopolar space-charge density (ρ) [8], [9], [30]. HVDC transmission lines are normally designed to operate in a bipolar configuration with a conductor bundle for each polarity. The electric field is due in part to the high voltages applied to the conductors. Copious amounts of ions are produced by corona at each conductor bundle, and the presence of the ions contributes significantly to the electric-field strength at ground level [9]. In the absence of wind, the ions travel along electric-field lines to the conductors of opposite polarity, to the ground wires, and to the ground plane. Depending on the air composition, a number of resultant ion species, each with its characteristic mobility, are formed following ion-molecule reactions by the primary ions that are initially produced by the corona. The drift velocity of each ion is equal to the product of its mobility and the electric-field strength. In the presence of wind, the ion velocity is given by the sum of the drift velocity and wind velocity ($\vec{v}_a$). The monopolar ion current density in this case is given by

$$\vec{I} = \rho K \vec{E} + \rho \vec{v}_a \tag{1}$$

where

K = the average ion mobility

The wind can be thought of as a perturbing influence because it causes temporal fluctuations in the values of ρ, and therefore $\vec{E}$ and $\vec{J}$, at a given point. In addition, when the wind velocity is comparable to or greater than the ion drift velocity, significant numbers of ions can leave the vicinity of the right-of-way and travel downwind from the transmission line. A schematic view of the electrical environment in the vicinity of an HVDC transmission line is shown in Fig 1, which is taken from [8]. For clarity, the influence of the air motion has been taken to be negligible. It is common practice to assume that the ions are singly charged and to calculate the monopolar ion number density from ρ [12]. A more complete description of the electrical environment near HVDC transmission lines is given in references [8], [9], [30]. It should be noted that, in general, dc electric fields with ions cannot realistically be modeled using 60 Hz electric fields because of the significant and often unpredictable influence of the ions that can vary the electric-field strength at a point because of wind action or by charging nearby insulator surfaces.

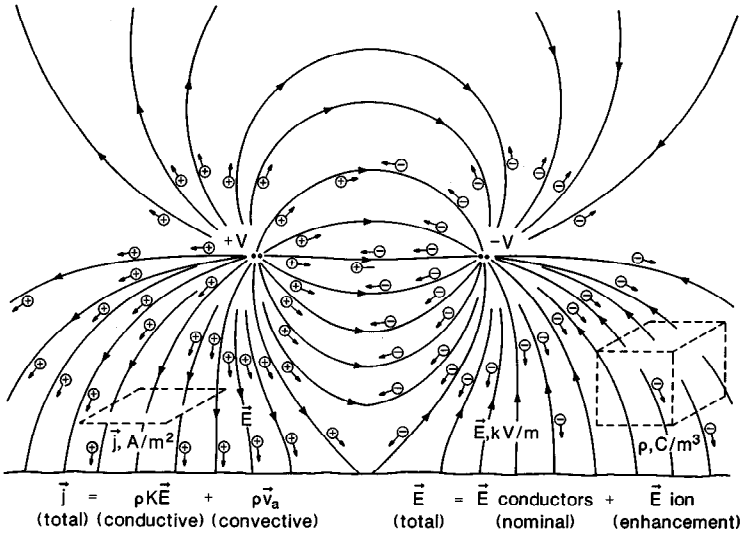

NOTE—Ions produced by corona at each conductor bundle travel along electric-field lines to the conductors of opposite polarity and to ground in the absence of wind.

Figure 1 — Schematic View of a Bipolar High-Voltage DC Transmission Line

6. Electric-Field-Strength Measurements

6.1 Instrumentation and Principle of Operation.

Two types of dc electric-field-strength meters are considered in this guide: field mills or generating voltmeters and vibrating plate electric-field meters (i.e., field meters employing probes that contain vibrating plates). Both devices determine the electric-field strength by measuring modulated, capacitively induced charges or currents sensed by metal electrodes. Other instrumentation for measuring dc electric fields in the presence of space charge have been reported in the technical literature,[3] but they are not considered here because of their specialized nature and/or their lack of availability.

6.1.1 Field Mill (Generating Voltmeter).

Two types of field mills are described in the technical literature, the shutter type and the cylindrical type. The more common is the shutter-type field mill, which has a sensing electrode that is periodically exposed and shielded from the electric field by a grounded rotating shutter. Shutter-type field mills are usually operated with the shutter nearly flush with the ground plane. The induced charge at any instant, q_s, as well as the induced current (i_s) between ground and the sensing electrode as the sensing electrode is alternately exposed and shielded, are proportional to the electric-field strength (E). That is,

$$\gamma_s(t) = \varepsilon_0 E a(t) \tag{2}$$

[3]See, for example, Tassicker, O. J. "Boundary Probe for Measurement of Current Density and Electric Field Strength—With Special Reference to Ionized Gases." *Proceedings of the IEEE*. vol. 121, 1974, pp. 213–220; Cooperman, P. "A New Technique for the Measurement of Corona Field Strength and Current Density in Electrical Precipitation." *Transactions of the American Institute of Electrical Engineers*. vol. 75, 1956, pp. 64–67; Hidaka, K. "A New Method of Electric Field Measurements in Corona Discharge Using Pockels Device." *Journal of Applied Physics*. vol. 53, 1982, pp. 5999-6003.

where

$\in_0$ = the permittivity of free space
$a(t)$ = the exposed area of the sensing electrode at time t

The induced current is found by taking the derivative of Eq 2:

$$_s(t) = \frac{dq_s(t)}{dt} = \frac{\varepsilon_0 E da(t}{dt} \quad (3)$$

Thus, the field strength can be determined by measurement of the induced charge, current, or voltage across an impedance that is located between the sensing electrode and ground. A simplified schematic view of a shutter-type field mill is shown in Fig 2.

If the induced-current signal is rectified by a phase-sensitive detector operating with a suitable phase angle relation to the motion of the shutter, the dc signal output will indicate the polarity and magnitude of the electric-field strength [61].

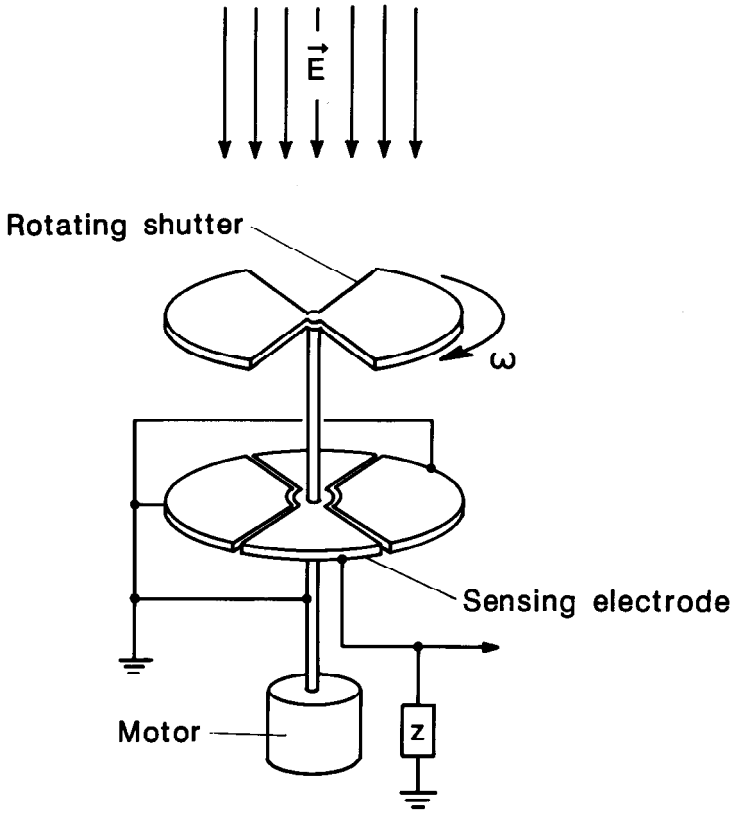

NOTE—The grounded rotating shutter periodically shields the sensing electrode, which leads to a time-varying current between ground and the sensing electrode.

Figure 2 — Simplified Schematic View of a Shutter-Type Electric Field Mill

Because of the presence of space charge in the vicinity of dc power lines, it is possible to have, in addition to the induced current, conduction current (of ions) to the sensing electrodes of the field meter. This additional current, which is chopped by the rotating shutter, represents an error signal and shall be corrected for in the instrumentation. One approach is to use phase-sensitive signal processing that discriminates against the conduction current, which is in quadrature with the induced-current signal [61].

While shutter-type field mills are normally operated in the ground plane in order to measure the field at ground level, measurements of the field at ground level can also be made with a field mill that is mounted on a stand, provided the measurements are corrected for the associated field enhancement through some calibration procedure (see *form factor* in Section 2). It should be noted that the geometry that exists during the calibration process shall be maintained during the measurements. For example, if grass or weeds are allowed to grow near the stand, the effective ground plane could rise. Similarly, the ground plane would be affected by the accumulation of snow on the ground. A method for establishing a well-defined ground plane for most weather conditions during measurements at ground level is described in 6.3.1.1.

During the measurements, the observer should be well removed from the measurement location to avoid perturbing the electric field. Some signal processing occurs in the housing that contains the sensing electrode and shutter. The remainder of the signal-processing circuit and field-strength display are contained in a shielded enclosure that is connected to the sensing electrode housing with a shielded cable.

Because the electric field in the vicinity of a dc power line is not uniform, it may be of interest to measure the electric-field strength at points above the ground plane. This can be done with the second type of field mill, the cylindrical field mill. Typically, the charges are induced by the electric filed on two exposed half-cylinder sensing electrodes. The induced charges on the sensing electrodes are varied periodically by rotating the sensing electrodes about the cylinder axis at a constant angular frequency, as shown schematically in Fig 3. Expressions for the induced charge (q_c) and current (i_c) between the half-cylinders for a cylinder of length L, ignoring end effects, are [39]

$$_{lc} = 4\varepsilon_0 r_0 LE \sin\omega_i \tag{4}$$

and

$$_{c} = 4\varepsilon_0 r_0 LE\omega \cos\omega_i \tag{5}$$

where

r_0 = the cylinder radius

Eq 4 and Eq 5 show again that measurement of the induced charge or current permits a determination of the electric-field strength.

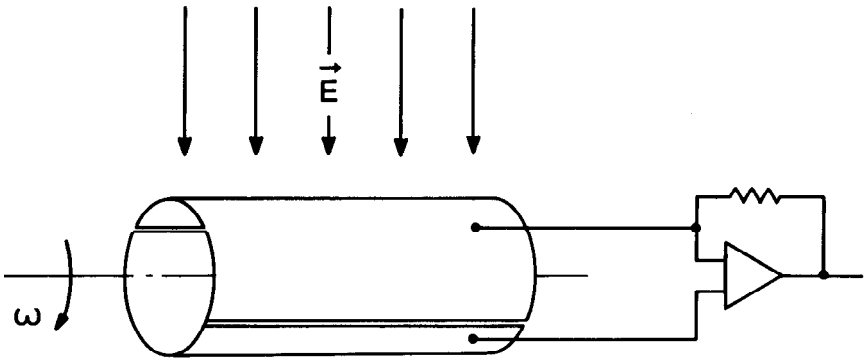

NOTE—The charge induced on each half-cylinder by the electric field is made to vary periodically by rotating the cylinder at a constant angular velocity.

Figure 3 — Schematic View of a Cylindrical Field Mill

Cylindrical field mills that operate at near space potential [37], [38], [43] and at ground potential [50] have been developed for measurements above the ground plane near dc power lines. For both cases, the field at the surface of the cylinder will be a superposition of two components, one due to the field from the dc power line (distorted by the cylindrical probe) and the other due to a constant, symmetrically distributed charge on the cylinder. Fig 4 schematically shows these two field components and the field resulting from their superposition for the case of a ground-referenced cylindrical field mill. Because no electrical signal is generated by the symmetrically distributed self-charge [Fig 4(b)] as the cylinder rotates [38], the signal that is produced is due to the time-varying induced charge or current approximately described by Eqs 4 and 5 and, as for the case of the shutter-type field mill, a time-varying ion current due to the space charge in the field. In order to determine the electric-field strength with both currents present, ground-referenced cylindrical field mills require two sets of rotating cylinders with different frequencies of rotation [50].

The picture corresponding to Fig 4 for an electrically isolated cylindrical field mill is similar, except that the self-charge uniformly distributed on the cylinder is of opposite polarity and results from a charging process due to ions in the field impinging on the cylinder. The cylinder becomes fully charged in a negligible time and prevents the further flow of ions to the sensing electrodes. Thus, the need for a second set of sensing electrodes rotating at a different frequency, as required for the ground-referenced cylindrical field mill, is eliminated.

The abbreviated account of field mills presented here is intended as a brief introduction. Since the first report of the shutter-type field mill by Harnwell and Van Voorhis in 1933 [27] and the cylindrical field mill by Kirkpatrick and Miyake in 1932 [44], numerous articles have been published[4] describing variations of the basic designs as well as methods for signal detection.[5]

---

[4]See, for example, Mapleson, W. W. and Whitlock, W. S. “Apparatus for the accurate and continuous measurement of the earth's electric field.” *Journal of Atmospheric and Terrestrial Physics*. vol. 7, 1955, pp. 61–72 and the references therein; Malan, D. J. and Schonland, F. J. “An Electrostatic Fluxmeter of Short Response-time for use in Studies of Transient Field-changes.” *Proceedings of the Physical Society.* vol. 63, pt. 6-B, 1950, pp. 402–408; Smiddy, M. and Chalmers, J. A. “The double field-mill.”*Journal of Atmospheric and Terrestrial Physics* vol. 12, 1958, pp. 206–210; Gathman, S. G. and Anderson, R. V. “Improved Field Meter for Electrostatic Measurements.” *Review of Scientific Instruments*. vol. 36, 1965, pp. 1490–1493; Collocot, S. J. “A Novel Method for Deriving the Reference Signal in Electric Field Mills.” *Journal of Electrostatics*. vol. 9, 1981, pp. 389–391.

[5]Use of a vibrating shutter rather than one that rotates is described in Horenstein, M. N. “Peak sampled vibrating-reed for the measurement of electric fields in the presence of space charge.” *Review of Scientific Instruments*. vol. 54, 1983, pp. 591–593.

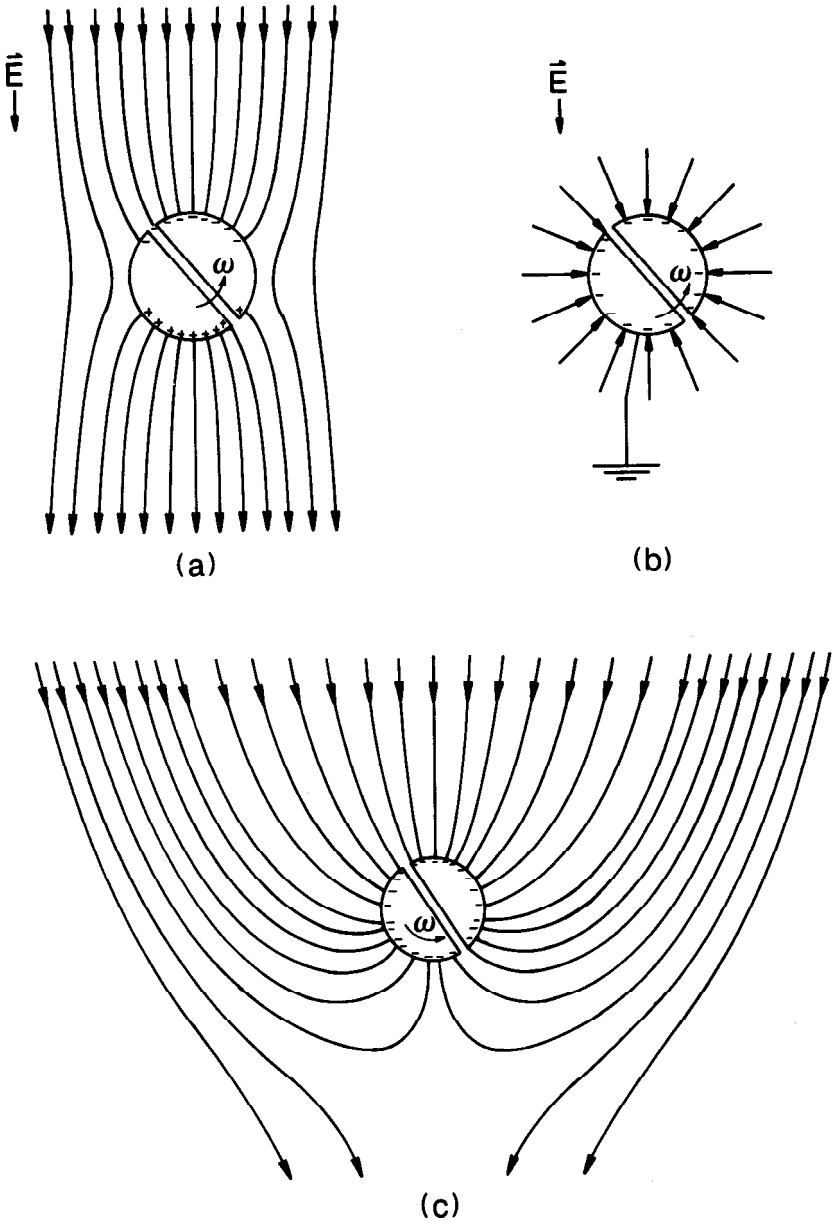

NOTES:
(a) An approximately uniform electric field distorted by an electrically isolated cylindrical field mill with indication of induced charges.
(b) A symmetric field near the surface of a grounded cylindrical field mill that is due to a uniformly distributed self-charge that originates from ground.
(c) Superposition of fields in (a) and (b) after [50]; detector responds to changes in induced charge as field mill rotates with angular frequency ω.

Figure 4 — Schematic View of an Electric Field Near the Surface of a Ground-Referenced Cylindrical Field Mill in a Nearly Uniform Electric Field

6.1.2 Vibrating Plate Electric-Field Meters.

In contrast to the literature on field mills, relatively few publications have appeared describing electric-field meters with vibrating plate probes [17], [18], [56], [68]. Fig 5 shows a simplified schematic view of a probe with a vibrating-plate sensing electrode. Charges induced on the plate below the aperture by the electric field are modulated by the vibrational action of the mechanical driver. For the configuration shown in Fig 5, the field meter responds to the negative charges induced on the vibrating plate by generating a negative feedback voltage, V_{fb}, to the faceplate to null the signal from the vibrating plate, V_s; the electric-field strength is proportional to the feedback voltage [68]. As in the case of the shutter-type field mill, the vibrating-plate probe is mounted flush with the ground plane during use, and a portion of the signal-processing circuit and field-strength display are located remotely in a shielded box. The observer should be sufficiently removed from the measurement location to avoid perturbing the electric field.

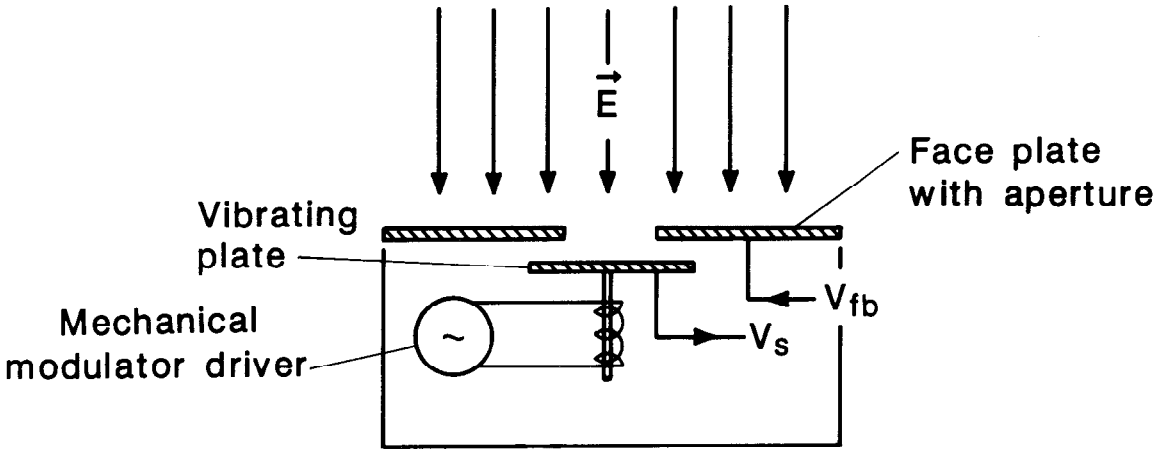

NOTE—The charge induced by the electric field on the sensing plate varies with time because of the vibrational motion.

Figure 5 — Schematic View of Vibrating. Plate Electric-Field Meter Probe

6.2 Calibration of Instrumentation.

Because of the presence of space charge in the vicinity of HVDC transmission lines (Section 5), a known dc electric field with space charge is desirable for calibration purposes. Other desirable features of an apparatus that generates the calibration field are that:

1) The region of uniformity is sufficiently large to reduce the uncertainty in the value of the field strength to an acceptable level at the location of the probe;
2) The electric field is not significantly perturbed by nearby objects, ground planes, or the operator performing the calibration; and
3) The dimensions of the apparatus are sufficiently large that the probe does not significantly perturb the charge distributions on the electrode surfaces producing the field.

Parallel plates can be used to generate known electric fields and also to satisfy the above criteria. Parallel-plate systems that can produce known electric fields with and without space charge are described in the following two sections. The apparatus that produces a field with space charge is more complicated in construction and operation than the space charge-free system. In addition, for ion-current densities and electric fields near HVDC transmission lines, i.e., $J < 0.1 \times 10^{-6}$ A/m^2 and $E > 10$ kV/m ([9], [17], [35]), the measurement

error due to space charge for some instrumentation may be negligible or small [56]. In such situations, the simpler space-charge free system described in 6.2.1 may be adequate for calibration purposes. Normal high-voltage safety practices should be observed during the calibration procedures [2].

6.2.1 Calibration Field Without Space Charge.

Regions of uniform field of known magnitude and direction without space charge can be created for calibration purposes with parallel plates, provided that the spacing of the plates, relative to the plate dimensions, is sufficiently small [59]. The uniform field value ($E0$) is given by V/d, where V is the applied potential difference and d is the plate spacing. The magnitudes of the normalized field, E/E_0, at the plate surface and midway between semi-infinite parallel plates are plotted as a function of normalized distance x/d from the plate edge in Fig 6. Metal sheets or tightly stretched metal screens can be used as parallel plates.

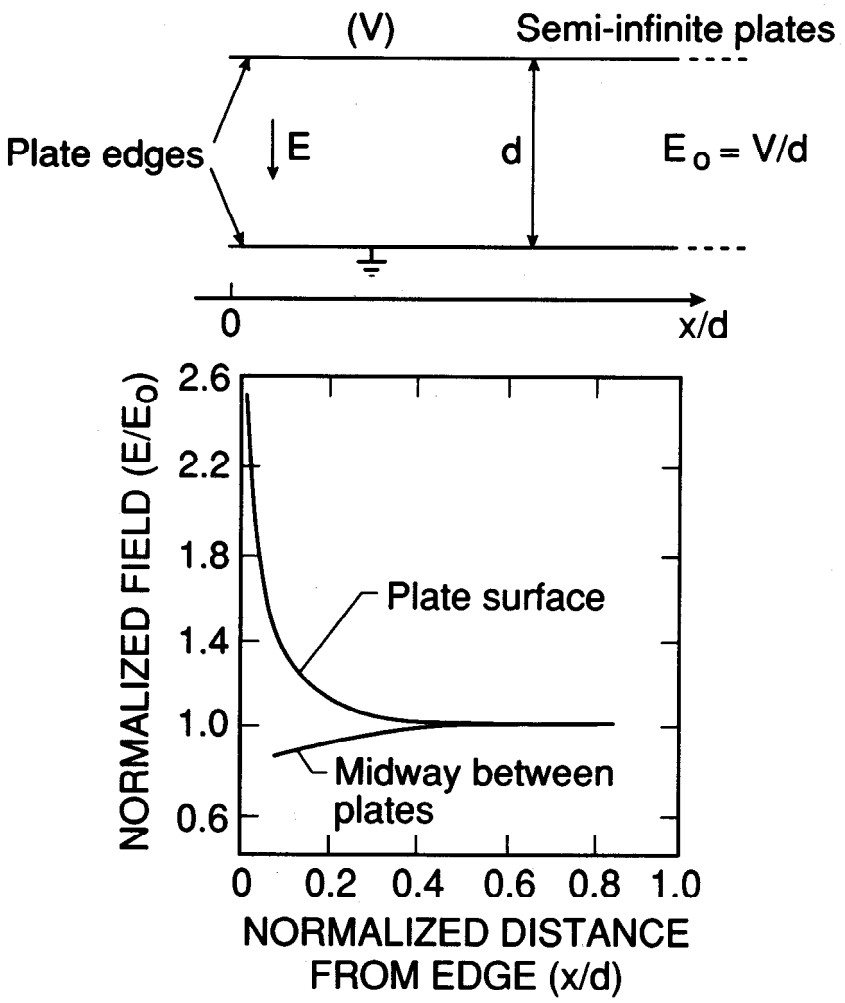

Figure 6 — Normalized Electric Field at the Surfaces of and Midway Between Semi-Infinite Parallel Plates

The curves in Fig 6 and the corresponding numerical values in Table I show that the departure from uniformity due to fringing field effects is 0.1% at a distance of one plate spacing from the edge. For square plates of finite size, the fringing field effects from four edges can be estimated by superposition when the effect

from each edge is less than 0.1%. Numerical calculations of fields between finite-size parallel plates suggest that a discrepancy of approximately 0.04% exists for estimates of fringing fields using the results in Table 1 for a distance of one plate spacing in from the edges of the parallel plates [65]. These results are valid in the absence of perturbations due to nearby grounded objects or planes.

Table 1—Normalized Electric-Field Strength Midway Between Plates and at Plate Surfaces

Midway Between Plates		Plate Surface	
x/d	E/E_0	x/d	E/E_0
0.0698	0.837	0.0185	2.449
0.1621	0.894	0.0829	1.414
0.2965	0.949	0.1230	1.265
0.4177	0.975	0.1624	1.183
0.6821	0.995	0.2431	1.095
0.7934	0.997	0.4376	1.025
1.0000	0.999	0.6861	1.005
		0.7954	1.002
		1.0000	1.001

6.2.1.1 Calibration in Ground Plane.

Electric-field meters that operate in the ground plane can be calibrated by making a hole in the center of the bottom plate and mounting the field-meter probe flush with the bottom plate. It is assumed that the hole is nearly filled by the probe. Shutter-type field mills may introduce small cavities in the ground plane (i.e., the shutter is flush with the ground plane and the sensing electrode is below the shutter). In this regard, it should be noted that the electric-field perturbation due to a circular hole in the ground plane decreases to 0.7% at a distance of three radii above the center of the hole [24], [58]. Thus, a parallel-plate spacing that is three times the radius of the hole made for a shutter-type field mill will conservatively eliminate significant perturbations of the surface-charge density on the top plate. To minimize perturbations of the electric field at the location of the probe by nearby ground planes and the stray field from the high-voltage lead to the energized plate, the outer edge of the sensing electrode (of the probe) should be no closer than two plate spacings to any edge of the grounded plate. The distance between the parallel plates and nearest ground plane (walls, floor, etc.) should be at least two plate spacings. Under these conditions, the calibration field can be calculated from the expression V/d with an uncertainty of less than 0.5% [55]. Uncertainties in the values of V and d will combine with the 0.5% uncertainty (square root of the sum of the squares). A check of instrument calibration during outdoor measurements is discussed in 6.4.

It is emphasized that the field-meter probe should be flush with the ground plane for precise calibrations and subsequent measurements. For example, a misalignment of one or two millimeters of a vibrating plate probe, relative to the ground plane, can lead to a change of several percent in the measured field-strength value.

6.2.1.2 Calibration Above Ground Plane.

Calibration of cylindrical field mills above the ground plane can be made by supporting the cylindrical probe centrally between the parallel plates with the handle normally used for measurements; the handle orientation (or fiber optic link), if adjustable, should be the same during calibration and subsequent measurements. From the data in Table 1, a parallel-plate system in which the side dimension of the plates (L) is twice the parallel-plate spacing (i.e., $L/d = 2$) will have a field at its center that will be within 1% of the uniform field value given by V/d in the absence of nearby ground planes.

The perturbation of the field between the plates by nearby ground planes can be minimized by balanced energization, i.e., using equal voltages of opposite polarity to energize the parallel plates. For such an arrangement and if $L/d = 2$, the influence of vertical ground planes one plate spacing away from the parallel plates will be negligible at the center of the parallel plates [46], [65].

The parallel-plate spacing should be sufficiently large so that perturbation of the calibration field by image charges in the parallel plates (proximity effect) will be negligible. Two types of image-charge effects should be considered. One effect, which is always present, is the field perturbation due to images of the induced charges on the cylindrical probe. The second effect is present if the cylindrical probe has a self-charge, which can occur if the field mill is a ground-reference device (see 6.1.1 and 6.2.2.2). An estimate of the error produced by image charges associated with the induced charges can be made by modeling the cylindrical probe as a rectangular box that encloses the cylindrical probe. Takuma et al. [65] have shown that for a rectangular box 10 cm x 10 cm x 8 cm high, centrally located in a parallel-plate system and for the condition $L/d = 2$, the error in percent due to the proximity of both plates can be expressed as $(v/8D^3) \times 100$, where v is the volume of the probe (box) and D is the distance between the center of the probe and each plate. The expression $(v/8D_3) \times 100$

has also been found to be useful for predicting the proximity effect of a probe with a “taller” geometry, 5.1 cm x 14 cm x 18.2 cm high.[6]

Image-charge effects due to a self-charge on a ground-referenced cylindrical field mill can be cancelled by positioning the probe midway between the parallel plates of the calibration apparatus. What remains is the image charge or proximity effect due to the induced charges discussed above.

An electrically isolated instrument can be calibrated above the ground plane in the same way as a ground-referenced device. However, if the field-meter probe is centrally located between the plates, the calibration procedure will not include a check on the adequacy of the coupling to the local space potential. If the insulating pole that supports the probe in the field is not scrupulously clean, there may be a leakage path to ground. The probe will then charge to ground potential, but the central location of the probe will lead to the cancellation of the field perturbation due to the image charges. To check for this effect, electrically isolated instruments that are being calibrated without the presence of space charge should be positioned asymmetrically between the parallel plates following calibration at a location midway between the parallel plates. Because of the nearly uniform electric field between the parallel plates, there should be no significant change in the reading of the field meter if the coupling to the local space potential is adequate.

The presence of a clean insulating pole in close proximity to the field-meter probe, as noted above, may lead to difficulties during calibration at ambient field levels, i.e., 120 V/m. The insulating surface can act as a trap for ambient space charge, and the trapped charge may significantly perturb the calibration field. The use of a radioactive ion source mounted on the pole may overcome this difficulty, but the radioactive source can introduce additional problems, as discussed in 6.3.3.

Uncertainties in the values of V and d and the uncertainty due to proximity effects should be combined (square root of the sum of the squares) with the 1% uncertainty resulting from fringing-field effects.

[6]See the discussion in [65].

6.2.2 Calibration Field With Space Charge.

A schematic view of an apparatus that can produce a calculable electric field with space charge is shown in Fig 7. Ions generated by stainless-steel corona wires are directed both upward (to the cap) and downward to the first screen. Ions not collected on the first screen continue downward to the second screen, which is the top "plate" of a parallel-plate system. The ions that pass through the top plate travel a distance d to the bottom plate and form the current density J. An electrometer is used to measure the ion current to electrically isolated current-sensing patches mounted on the bottom plate. Knowledge of the area of the patches then permits the calculation of J. The side dimensions of the parallel plates are 1.7 m x 1.7 m, and the spacing can be made as large as about 25 cm.

The solution of Poisson's equation in one dimension yields expressions for the electric field strength, $E(z)$, and electric space potential, $\phi(z)$, between the parallel plates [56]:

$$E(z) = \left[E_t^2 + \frac{2J(d-z)}{K\varepsilon_0}\right]^{1/2} \tag{6}$$

$$\phi(z) = V_t - \left(\frac{K\varepsilon_0}{3J}\right)\left[\left(E_t^2 + \left(\frac{2J(d-z)}{K\varepsilon_0}\right)\right)^{3/2} - E_t^3\right] \tag{7}$$

where

z = the distance above the bottom plate
V_t = the potential of the top plate ($z = d$)
E_t = the electric field at the top plate
K = the average mobility

Following procedures described in [56], the values of K and E_t can be determined experimentally, thus permitting the calculation of E from Eq 6 for a given current density. Electric-field-strength values can be calculated with an uncertainty of less than ±2% [56].

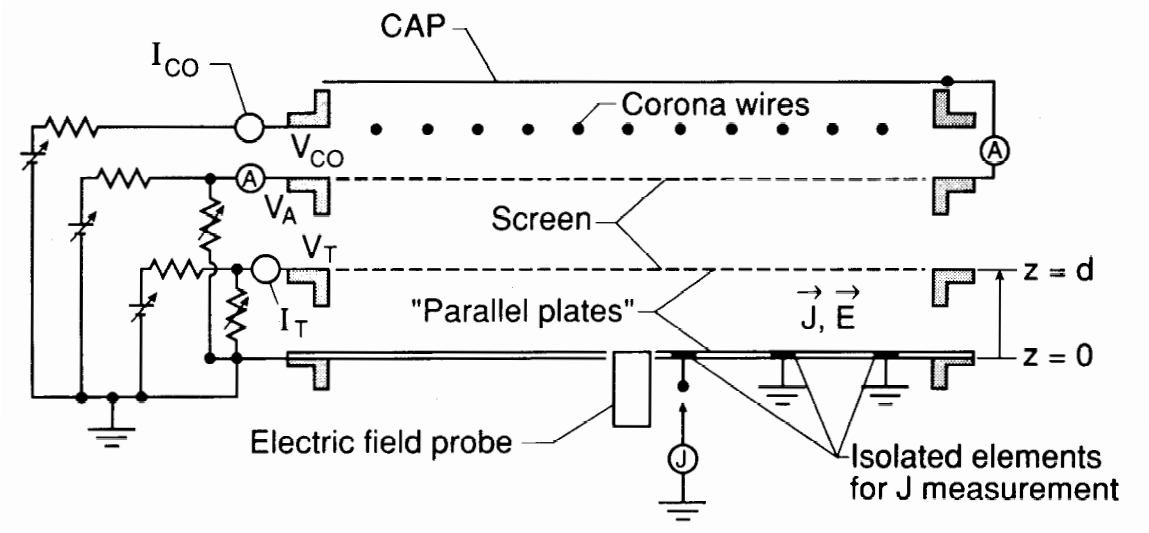

NOTE—The arrangement shown is appropriate for generating an electric field with positive ions. The corona wires are oriented parallel to one another and perpendicular to the plane of the figure. Further details of the apparatus are given in [56].

Figure 7 — Schematic View of a Parallel-Plate System That Produces DC Fields With Ions

6.2.2.1 Calibration in Ground Plane.

Electric-field meters that operate in the ground plane can be calibrated by making a hole in the center of the bottom plate and mounting the field-meter probe flush with the bottom plate. It is assumed that the hole is nearly filled by the probe. Shutter-type field mills may introduce small cavities in the ground plane. In this regard, it should be noted that the electric-field perturbation due to a circular hole in the ground plane decreases to 0.32% at a distance of four radii above the center of the hole in the absence of space charge [24], [57], [58] and somewhat more with the presence of space charge [57], [58]. Thus, a parallel-plate spacing that is four times the radius of the hole made for a shutter-type field mill will conservatively eliminate significant perturbations of the surface-charge density on the top plate.

It is emphasized that the field-meter probe should be flush with the ground plane for precise calibrations and subsequent measurements. For example, a misalignment of one or two millimeters of a vibrating-plate probe, relative to the ground plane, can lead to a change of several percent in the measured field-strength value.

6.2.2.2 Calibration Above Ground Plane.

Calibration of ground-referenced or electrically isolated cylindrical field mills that operate above the ground plane can be made by supporting the cylindrical probe at the center of the parallel plates with the handle normally used for measurements. If the orientation of the handle (or fiber-optic link) can be varied relative to the probe, the orientation during calibration should be the same as that during measurements. The spacing of the parallel plates must be sufficiently large that interactions between the probe and plates (i.e., image charges) can be considered negligible. For example, it has been shown, using a self-charged infinite cylinder model (see 6.1.1), that interactions with only the ground plane affect the field-meter reading by less than 10% if the distance between the center of the cylinder and ground plane is more than five times the cylinder radius [38]. This result is somewhat conservative because of the infinite cylinder approximation and ignores the much smaller image-field effects due to the induced charges on the cylinder.

However, if the field mill is centrally located between the electrodes of the parallel-plate apparatus, the image fields due to the self-charge will cancel, and the perturbation of the field is limited to that of the image fields associated with the induced charges on the cylindrical field mill. Image-charge perturbations of the calibration field due to induced charges on the field-meter probe are discussed further in 6.2.1.2.

For calibrations in a parallel-plate system containing space charge, the height of the cylinder shall be carefully determined because the value of the field is a function of distance above the ground plane (Eq 6).

6.3 Measurements

6.3.1 Power Line Electric-Field-Strength Measurements.

The measurement of lateral profiles of electric-field strength is generally considered a valid procedure for characterizing power-line electric fields. The lateral profile for an ac power line can be readily determined within minutes using a free-body field meter, a survey type device that permits measurements at most points above the ground plane [4], [22]. Subsequent departures of the field strength from the measured profile values are usually small for the same electrical load and temperature conditions (sagging of the conductors during warm days, heavy icing, or heavy electrical loads can significantly affect the electric-field strength).

In contrast to the ac power-line case, characterization of the dc electric-field strength near a dc power line is a more time-consuming and complicated process. Because of large variations in the electric-field strength due to such factors as rain, fog, snow, wind, ice, relative humidity, and fair weather seasonal effects, it has been found useful to represent the electric-field strength as a statistical quantity arrived at after measurements have been performed over an extended period.[7] To interpret the data properly, the weather-related parameters shall be recorded simultaneously with the electric-field-strength measurements. For example, the

use of instrumentation for the measurement of wind speed and direction, precipitation, and temperature would be desirable during measurements of the electric field. A meaningful presentation of the data requires an indication of such parameters at the time the data were obtained. For example, the maximum, minimum, and average field-strength values of the lateral profile could be presented for fair-weather or for "all-weather" conditions. The average and extreme values of the electric-field strength will likely differ for the two cases.

The more comprehensive the requirements of a measurement program are, the greater will be the duration of the measurement period. Electric-field-strength measurements near dc power lines have been reported for periods extending from days and weeks to many months.[8] The instrumentation for the short-duration measurement programs are typically portable, may be less automated, and are moved from point to point to obtain the data. Measurements that extend over many months are performed with instrumentation, frequently unattended, that is permanently positioned at several locations near the power line for simultaneous observations. Because the instrumentation is exposed to harsh environmental conditions, the maintenance and calibration requirements for the latter situation are much greater. A discussion of the problems that can be encountered and the measures taken for their correction is given by Chartier et al. [16].

While examples of long-term lateral profile measurements are presented in the next section, it is noted that data indicating the cumulative frequency or probability distribution of the electric-field strength at a given point have also been reported as a means for characterizing the electric-field environment near dc power lines [16], [28], [49].

It is noted that many of the techniques for measuring electric fields near dc power lines are applicable to areas outside a converter station building where electric fields with space charge may exist. Measurement of the electric field inside a converter station building where there is negligible space charge is discussed in 6.3.2.

6.3.1.1 Ground-Plane Measurements.

Lateral profile measurements of the electric-field strength in the ground plane beneath dc power lines may be reported in terms of the median field-strength value as well as, for example, the 5% and 95% values. The 5% and 95% values have been regarded by some researchers as practical minimum and maximum values for specific weather conditions. Other investigators have considered the $L_{0.5}$ exceedance level during all-weather conditions as a possible working maximum (exceedance levels have been used during measurements of corona phenomena such as radio noise and audio noise). The reliability of an $L_{0.5}$ exceedance level during measurements of the electric field depends greatly on the absence from the data base of measurement artifacts due to such things as transients in line operation(e.g., switching transients) or malfunctions in the operation of the instrumentation. Fig 8, taken from [35], shows examples of three lateral electric-field profiles measured at ground level for fair weather, fog, and rain conditions. The results were obtained with 13 electric-field-strength meters located at midspan along a straight line perpendicular to the conductors. To acquire this kind of data, measurements must be made as frequently as once every minute over a period of many months. This is most conveniently accomplished with an automatic data acquisition and storage system under computer control. Automated measurements of other relevant parameters such as climatic conditions are required in order to properly interpret the data [17], [23], [35]. Conductor geometry, line voltage, and time should also be recorded. An approximately flat area, free from towers, trees, fences, tall grass, and other irregularities, is recommended as the measurement site.

While the lateral profile measurements shown in Fig 8 represent electric-field-strength values in the ground plane, the instrumentation used to obtain the data were elevated vibrating-plate probes (see 6.1.2) with the sensing electrodes pointed at the ground. The responses of the inverted probes were calibrated by comparing readings during fair weather with field meters mounted flush with the ground plane in the usual manner [17]. This measurement approach reduces the perturbing effects of vegetation, insects, precipitation, and flooding.

[7]See [9], [17], [20], [23], [35], and [49].
[8]See [9], [16], [17], [23], [28], [35], and [49].

Another approach that has been used for reducing the effects of vegetation, insects, and flooding is to construct a large, slightly elevated, artificial ground plane (3.6 m x 11.0 m) using wire mesh nailed to a wooden frame [16]. The electric-field meter is then mounted flush with the ground plane with other instrumentation for measuring ion-current density (see Section 7) and monopolar charge density (see Section 9). Black plastic placed on the earth beneath the mesh discourages the growth of weeds.

If the field meters used for measuring the ground-level electric-field strength are permanently mounted flush with the ground plane, some provision should be made for draining rain water from the below-ground cavities that house the field meters and associated circuits. For example, sump pumps have been used for removing water from holes that house ion counters [16]. Mounting the field meter so that it is centrally located and flush with the surface of a Wilson plate operating in the ground plane (see Section 6) allows for more precise correlations between the electric-field strength and ion-current-density measurements.

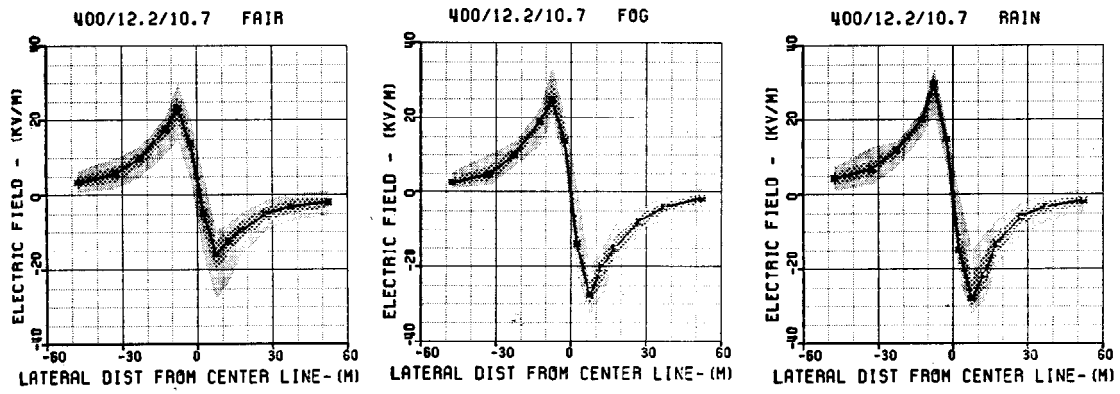

NOTE—The median electric-field strength values are indicated with solid curves. The 25 to 75 percentile field values are indicated with heavy shading, and the 5 to 95 percentile field values with light shading.

Figure 8 — Lateral Electric-Field Profiles Measured at Ground Level for Fair Weather, Fog, and Rain Conditions

It should be noted that the convention in describing electric fields near dc power lines is to designate the electric field into the ground as positive, i.e., the electric field under the positive conductor is considered positive.

The influence of an ac power line sharing the same right-of-way as a dc power line is discussed by Maruvada and Drogi [51].

6.3.1.2 Above-Ground-Plane Measurements.

Due in part to the lack of commercial instrumentation and difficulties associated with field-meter calibration in the presence of space charge (see 6.2.2 and 6.2.2.2.), only one above-ground lateral profile measurement has been documented and is described in a report by Kirkham and coworkers [43]. Instrumentation designed for electric-field-strength measurements above the ground plane are described in papers by Smiddy and Chalmers [62], Gathman [25], Maruvada et al. [50], and Kirkham and coworkers [37], [38], [43]. The cylindrical field mills described in [37], [38], [43], and [50] contain circuit elements that provide position-reference signals that permit the determination of the electric-field direction as well as the magnitude.

Above-ground measurements of the electric-field strength near a HVDC test line using cylindrical field mills with fiber optic links to detector circuits are described in [37], [38], [43]. Short-term measurements of the electric-field strength above the ground plane show good correlations with nearby simultaneous ground-plane measurements. Therefore, once a relationship is established between the above-ground and ground-plane measurements, the electric-field strength at the above-ground location can be monitored “remotely” using the field meter in the ground plane.

6.3.2 Indoor Electric-Field-Strength Measurements.

Because of the absence of certain outdoor environmental effects such as wind, rain, and fog, and the relatively small variation of such parameters as relative humidity and air composition in indoor settings, the electric-field strength is expected to remain relatively constant for a given electrode geometry and voltage level. For such cases, short-term measurements of the electric-field strength in and above the ground plane are expected to reflect the nominal long-term electric-field values. This assumes that there are no nearby objects or surfaces that can become charged in a poorly defined manner (e.g., insulating surfaces) and perturb the electric field in an unpredictable way. It is also assumed that the electrical parameters associated with field and ion-generating processes (i.e., electrode geometry, voltages, etc.) are time invariant.

6.3.3 Above-Ground-Plane Electric-Field Measurements in the Absence of Space Charge.

Measurements of the dc electric-field strength above the ground plane can be made in a space-charge-free environment (e.g., near electrical apparatus such as wall bushings, insulators, and surge arresters) with ground-referenced and electrically isolated cylindrical field mills. Because of the self-charge on the ground-referenced instrumentation, measurements near conducting surfaces can be affected by fields produced by image charges in the conductors [38]. To a lesser degree, image-charge fields due to the induced charges on the cylindrical field mill also influence the measurement.[9] The resultant effect of the image-charge fields is that the measured electric-field strength at a point exceeds the field value that existed there prior to the introduction of the cylindrical field probe. Approximate values of the errors due to the images of self-charge for an infinite cylinder are discussed in [38].

Because of the absence of space charge, electrically isolated cylindrical field mills do not, in principle, develop a self-charge, and the perturbation of the electric field is limited to the much smaller effect of image charges of the induced charges on the cylindrical probe. In prototypes of electrically isolated instrumentation developed by Kirkham et al, optical fibers have been used for transmission of electrical signals from the cylindrical probe to the field-strength display circuit. However, difficulty has been experienced in maintaining adequate insulation between the probe and ground. Resistances on the order of 10^{12} Ω have been found to be insufficient for preventing the probe from eventually reaching ground potential [38]. Image fields due to the self-charge of the probe then become a problem (see 6.2.2.2).

The problem of coupling the probe to space potential can reportedly be solved by means of a radioactive polonium ion source attached to the end of the insulating handle normally used to support the cylindrical probe in the electric field [38]. However, this procedure may result in charge accumulating on the probe, again leading to image-charge field effects. In addition, nearby insulators may become charged by ions produced by the radioactive source, causing a further perturbation of the electric field.

Above-ground electric-field measurements have been performed near outdoor dc insulators as part of a study to understand mechanisms for flashover across insulator surfaces [42]. Because of the absence of space charge and the use of an electrically isolated cylindrical field mill during the measurements, image-field perturbations were reportedly minimized, and field strength measurements near the insulator surface were made possible. However, in light of the possible problems cited above of surfaces charging due to the radioactive element, additional studies appear necessary to better define the uncertainty associated with this measurement approach.

6.4 Sources of Measurement Error.

Instruments used outside the laboratory to monitor the long-term performance of a dc power line are usually subjected to severe environmental conditions that may affect the operation of the device and the accuracy of

[9]The image-charge field effects for induced charges on a finite-length cylindrical probe remain to be determined. The problem for a spherical dipole is described in Cooke, C. M. “Proximity Effect of a Conducting Plane In Electro-Optic Field Probe Measurements.” *1983 Annual Report, Conference on Electrical Insulation and Dielectric Phenomena*. Buck Hill Falls, PA, pp. 104–109.

the measurements. Under these conditions, reliable measurements will be obtained only if methods of periodically checking instrument operation, calibration, and drift are considered as part of the measurement protocol [16].

Because of the possibility of charge accumulation on insulating surfaces during outdoor and indoor measurements, these surfaces should not be exposed to the electric field. Charge accumulation can result in measurement instability and in long-term drift. For example, charging of the underside of the rotating shutter of a field mill because of surface contamination can result in instabilities or a systematic shift in field values. Similar effects may occur if surfaces within the housing of a vibrating-plate probe become charged [9]. Increasing the spacing between the shutter and sensing electrode on the field mill and using a pressurized air-purging system in the vibrating-plate probe [17] help to reduce these effects.

Because of harsh outdoor environmental conditions, it is possible that electrically sensitive metal surfaces will become corroded and acquire a charge. As with charged insulating surfaces, this can lead to instrument drift and instability. The likelihood of these problems can be reduced by gold-plating the metal surfaces.

Under conditions of large ion-current densities, in excess of those normally encountered under dc power lines, vibrating-plate field meters may indicate field-strength values that are too low because of a mechanism associated with a large impedance between the vibrating plate and ground [56].

As noted in 6.2.1.1, field meters should be flush with the ground plane when used for measurements at ground level. Field probes that project above the ground plane will indicate excessively high field values; if the probe is positioned below the ground plane, the indicated field values will be too low.

Raindrops can short-circuit elements in electric-field probes and disrupt measurements. Elevating field mills and vibrating-plate probes above the ground plane and inverting them so that they point toward the ground [26], [35] reduces the likelihood of the short-circuit problem. The responses of the probes used in this manner to obtain the data in Fig 8 (see 6.3.1.1) were calibrated by comparing readings with a field meter mounted flush with the ground plane [35]. However, it should be noted that the calibration will depend in part on the spatial distribution of charge density. For example, if the calibration of the inverted field meter is performed in the absence of space charge, some measurement error will likely occur if the field meter is later used when there is a layer of space charge near ground level [26].

Shutter-type field mills operating in the ground plane have been successfully used during rain, fog, and snow by incorporating heating elements in the probe. A shutter frequency of 180 Hz in combination with a 180 Hz tuned filter in the signal-processing circuit minimized unwanted noise signals produced by charged moisture particles discharging on the stationary sensing electrode [16].

The calibration of shutter-type field mills mounted flush with the ground plane can be checked with parallel plates by placing an energized plate above the field mill and using the ground plane as the bottom plate of a parallel-plate system. Refer to 6.2.1.1 for appropriate plate dimensions and spacing. A portable, battery-operated parallel-plate system has been used for such outdoor calibrations [16].

Observer proximity effects during measurements in the ground plane can lead to attenuated field strength in the absence of space charge and possibly enhanced field-strength values when there is space charge present. In general, proximity effects are a function of distance between the observer and measurement location, measurement height above ground, and the electric potential of the observer, e.g., grounded or elevated potential because of charging [4], [9], [21], [22].

7. Current-Density Measurements

7.1 Instrumentation and Principle of Operation.

Measurements of the vertical component of the ion-current density *J* in the vicinity of dc power lines are performed with a fiat collecting plate-electrometer combination. The flat plate, historically referred to as a Wilson plate [13], is located flush with the ground plane as shown schematically in Fig 9. The current density, averaged over the area of the plate (A), is given by

$$J = \frac{I}{A} \tag{8}$$

where

I = the measured current

The Wilson plate is isolated from ground but is held at ground potential via the electrometer circuitry. Wilson plates 1 m x 1 m, usually with guard bands to reduce fringing-field effects, have commonly been employed for current-density measurements near dc power lines [9], [17], [18], [20]. If necessary, the sensitivity of the current-density measurement can be increased by increasing the area of the Wilson plate.

Wilson plates that are smaller in dimension than the 1 m^2 devices used outdoors can be employed in indoor settings. For example, Wilson plates 10 cm x 10 cm x 0.157 cm thick have been fabricated from copper-clad printed circuit boards and used to measure *J* in the parallel-plate apparatus shown in Fig 7 [54]. The miniature Wilson plates rest on the surface of the ground plane rather than flush with it, and appropriate corrections need to be applied.

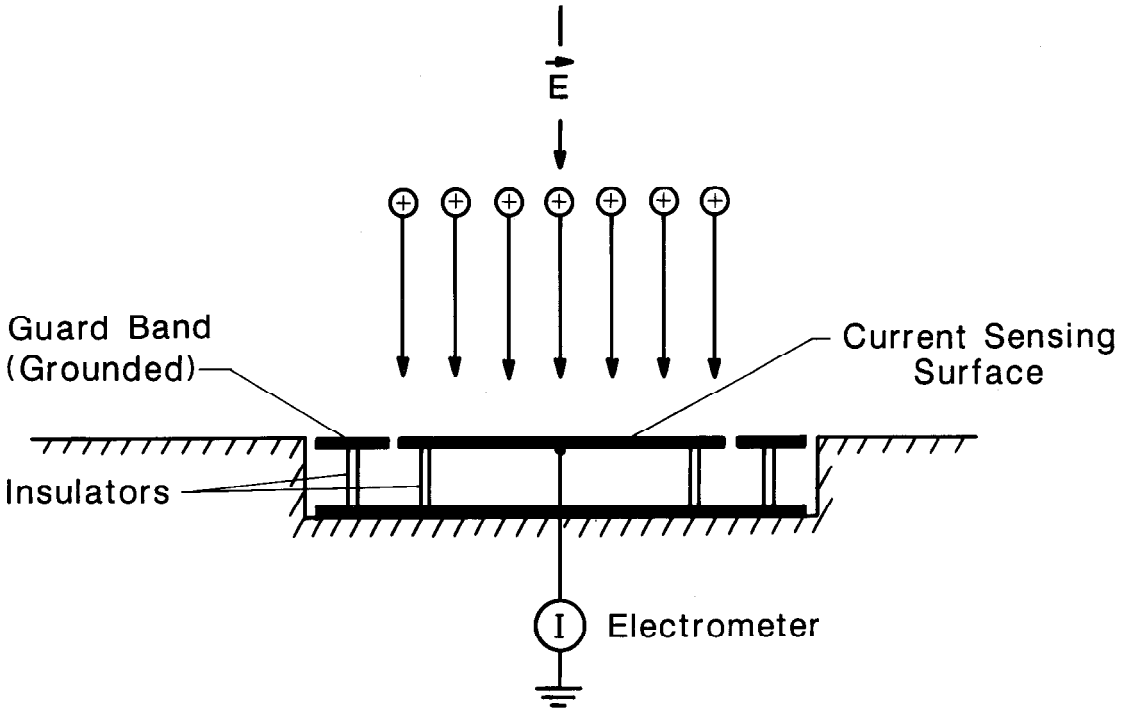

Figure 9 — Schematic View of a Wilson Plate Mounted Flush With the Ground Plane

7.2 Calibration of Instrumentation.

Calibration of a Wilson-plate measurement system requires knowledge of the uncertainties in the values of the sensing area (A) and measured current (I) in Eq 8. The uncertainty in the value of A for a Wilson plate can be made smaller by reducing the gap spacing between the plate and the guard band and assuming the "effective" ion collecting area of the plate extends to the midpoint of the gap. The electrometer can be calibrated with a current injection circuit consisting of an appropriately high-standard resistor, dc power supply, and accurate voltmeter. Fig 10 shows a simplified schematic view of the calibration circuit; the current is calculated from Ohm's law, $I = V/R$. It should be noted that the electrometer input is operated at virtual ground potential during calibration and subsequent current-density measurements. Measurement uncertainties in the values of A and I should be combined (square root of the sum of the squares) and reported as the total measurement uncertainty.

Miniature Wilson plates that rest on the surface of the ground plane (see 7.1) can be calibrated with 60 Hz electric fields in a parallel-plate apparatus and used for measuring J in indoor settings that simulate the dc power-line electrical environment [54], [55].

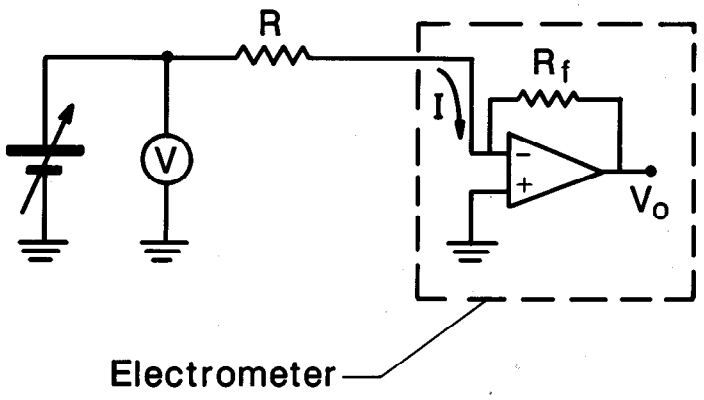

Figure 10 — Schematic View of a Current Injection Circuit for Calibrating Electrometer Used With Wilson Plate

7.3 Measurements

7.3.1 Power-Line Current-Density Measurements.

Much of the discussion regarding power-line electric-field strength measurements in 6.3.1 applies to ion-current density measurements, and the reader is encouraged to review the earlier section. Briefly:

1) Lateral profiles can be used to characterize the ion current density.
2) The data can be obtained over an extended period to determine the maximum, minimum, and median current-density values for specified weather conditions.
3) An automatic data acquisition and storage system monitors the current-density signals from permanently installed Wilson plates and from sensors indicating weather conditions.
4) The measurements represent current-density values at ground level.
5) The measurement techniques are applicable to areas outside a converter station building where significant levels of space charge may exist.

Short-term measurements with perhaps less automated, portable instrumentation, lasting less than a week, can also be performed in cases where a comprehensive data base is not required [9], [49].

Fig 11 shows lateral ion-current-density profiles obtained for the same weather conditions, line voltage and geometry, and time interval as for the electric-field-strength profiles shown in Fig 8. The Wilson plates used to obtain the data in Fig 11 were elevated 24 cm above the ground plane to avoid problems with precipitation, vegetation, and insects. The enhanced current-density values resulting from elevating the Wilson plates have been corrected to ground-level values [35] (see 7.4).

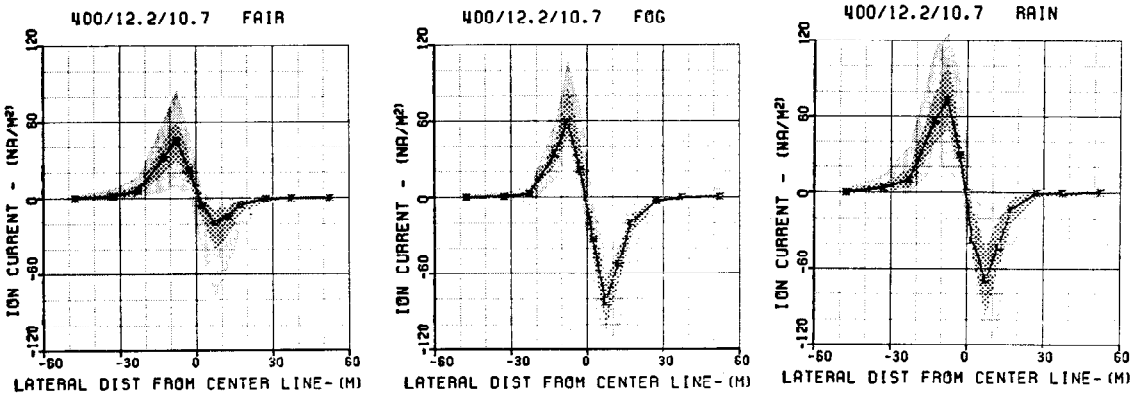

NOTE—The median ion-current-density values are indicated with solid curves. The 25 to 75 percentile values are indicated with heavy shading, and the 5 to 95 percentile values are indicated with light shading.

Figure 11 — Lateral Ion-Current-Density Profiles Measured at Ground Level for Fair Weather, Fog, and Rain Conditions

7.3.2 Indoor Current-Density Measurements.

Most of the discussion in 6.3.2 regarding indoor electric-field-strength measurements applies to indoor current-density measurements. For example, in the absence of nearby surfaces and objects that can become charged in an unpredictable way, short-term measurements of the ion current density in the ground plane are expected to reflect the long-term nominal current-density values. Miniature Wilson plates (see 7.1 and 7.2) may be more convenient for short-term measurements and will provide greater spatial resolution than the 1 m^2 device commonly used near dc power lines.

7.4 Sources of Measurement Error.

The precautions of periodically checking instrument operation, calibration, and drift as part of the measurement protocol during extended outdoor electric-field-strength measurements apply also to ion-current-density measurements [16].

Although the measurement of ion-current densities appears straightforward, systematic errors can affect its accuracy. If the electric field at the surface of the collecting plate changes due to the sudden shift of a cloud of charge overhead, then a displacement current results that is indistinguishable from the conduction current. Techniques for compensating for signals that result because of changes in the electric field at the surface of the sensor have been described in the literature. These techniques include integrating the current over known time periods to determine the average current [9], [16], use of special impedance matching [40], and simultaneous measurements of the electric field and suitable subtraction of the displacement current from the total current [33]. With the data acquisition system used to acquire the lateral profiles shown in Fig 11, time aver-

aging provides a median value of *J* that is nearly free of displacement-current effects. However, maximum and minimum values of *J* can still be influenced by displacement currents.

Errors that result when the Wilson plate is located above the ground plane for practical reasons, such as to eliminate effects of vegetation, precipitation, and insects, can be significant. In this case, there is an enhancement of the electric-field strength and ion current at the surface of the Wilson plate as shown schematically in Fig 12.

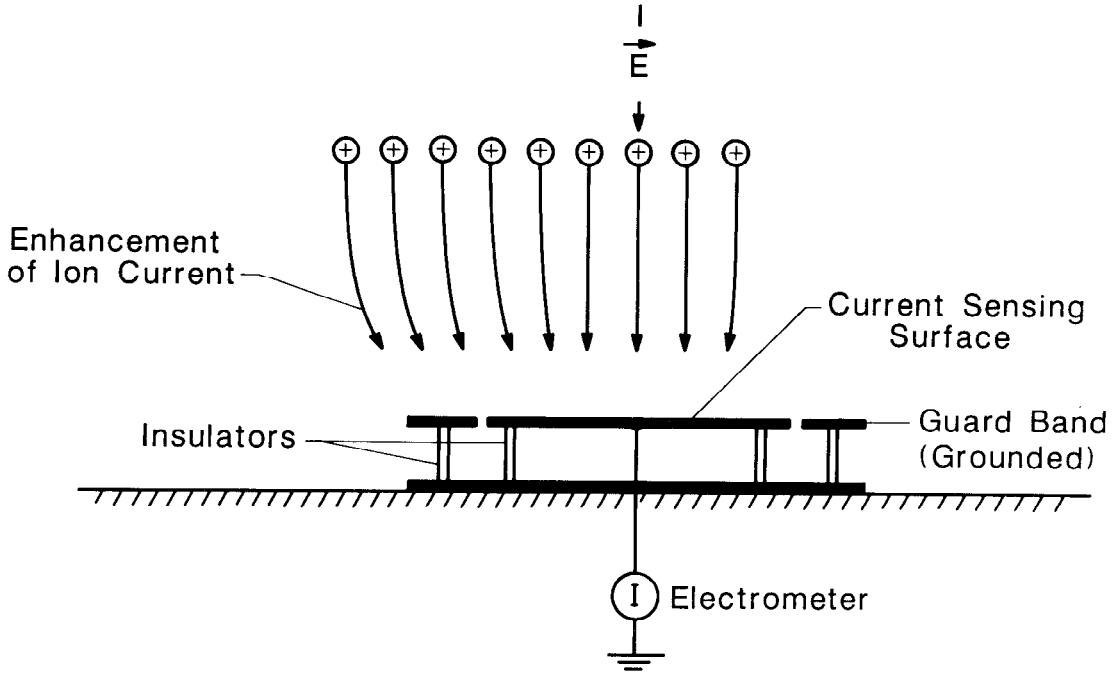

NOTE—The geometric enhancement of the electric field for this configuration results in an excessive ion current reaching the current sensing surface.

Figure 12 — Schematic View of a Wilson Plate Resting on the Ground Plane

A systematic study has been done to determine the errors associated with above-ground measurements of vertical current density [54]. This investigation was done primarily in the laboratory using various miniature Wilson plate geometries, but also included actual field data taken under a test line. The results of the study are summarized in Fig 13. While use of a guard band reduces the amount of "excess" current measured, the error associated with determining *J* can still be large. Geometric enhancement values for a given Wilson plate configuration were determined using both ac (60 Hz) electric field, and dc field and ion methods. For the conditions to be expected under a HVDC transmission line, the two methods give the same results, as in shown in Fig 13. In the figure, the solid curves represent composite data obtained using ac techniques, while the dc results are shown as discrete data points. Therefore, for a given Wilson plate configuration, the geometric enhancement factor can be determined using a parallel-plate system energized with a 60 Hz power supply [54], [55].

The accumulation of snow or ice on the Wilson plate or insulating surfaces can adversely affect its operation. Heating elements built into the Wilson plate have been used to prevent the accumulation of snow and ice [23]. Heating elements should also minimize leakage currents across insulating spacers. Use of a single insulator at the center of the sensing plate, creating an umbrella effect, has been found to be helpful in reducing leakage currents between the sensing plate and ground [16].

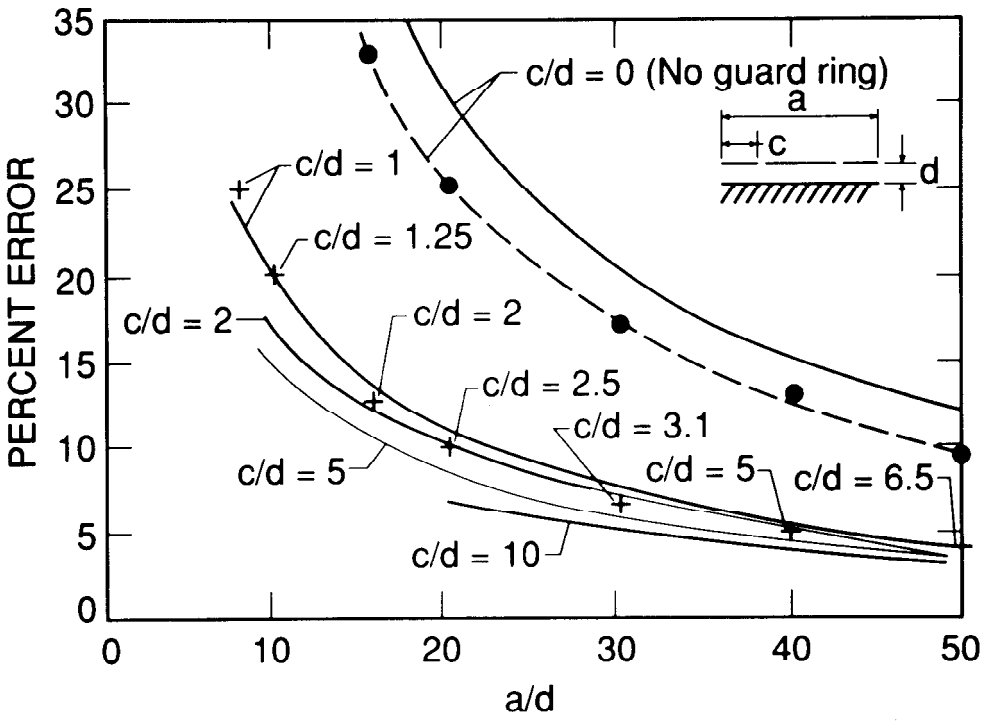

NOTE—Parameters a, c, and d are indicated on the figure. Solid curves are drawn through data points obtained by using ac fields to determine field enhancements. The symbols + and · indicate data points for dc fields with ions. DC operating conditions were comparable to those found under operating HVDC transmission lines

Figure 13 — Errors for Current Sensors Located above the Ground Plane .

8. Conductivity Measurements

Although conductivity measurements are not usually made near dc power lines, discussion of the instrumentation and principle of operation provides a useful introduction to ion measurements involving air flow and, in particular, the monopolar charge-density measurement, which is considered in Section 9.

8.1 Instrumentation and Principle of Operation.

The electrical conductivity of air, λ, can be determined by measuring, independently, the ion-current density and electric-field strength at a point in the absence of wind effects and calculating the ratio J/E.

$$J = \lambda E \tag{9}$$

Comparing Eqs 1 and 9, the conductivity can be expressed as a product of charge density and average mobility, ρK.

Conductivity may also be measured directly by using a cylindrical aspiration device known as a Gerdien tube,[10] which is illustrated in Fig 14. In the configuration shown, ions move under the influence of the air stream and the electric field established by the polarizing potential. Some fraction of the ions is deposited on the inner cylinder. Either positive or negative ions are collected, depending on the polarity of the polarizing

[10]See [12], p. 196.

potential, and the monopolar conductivity associated with these ions is measured. The solid curve in Fig 15 indicates, schematically, the current-voltage (*I-V*) characteristics of a Gerdien tube for a fixed flow rate through the instrument with no fringing electric-field effects (see 8.4). If the voltage and current are proportional (Ohm's law is satisfied), a measure of conductivity can be obtained. For certain operating conditions, i.e., decreased flow rate or increased polarizing potential, a saturation condition results, as indicated in Fig 15. By writing an expression for the current in terms of physical parameters, this behavior can be described analytically in the following way:

$$= M_0 e\left(\int_0^{k_c}\left(\frac{k}{k_c}\right)f(k)dk + \int_{k_c}^{\infty} f(k)dk\right) \tag{10}$$

$$k_c = \frac{M_0\varepsilon_0}{VC}$$

where

C = the effective interelectrode capacitance of the Gerdien tube
V = the polarizing voltage
M_o = the laminar volumetric air flow rate

The critical mobility, k_c, is the limiting mobility value for those ions that are completely collected by the Gerdien tube. All ions with mobilities $k > k_c$ will be collected, while only a fraction of those with mobilities $k < k_c$ will contribute to the measured current. In this expression for the current to the inner electrode, the expression $f(k)$ is the mobility distribution function and $f(k)dk$ is the number of ions with mobility between k and $k + dk$. The charge on an electron is e, and $\in_0$ is the permittivity of air. It is assumed that all ions are singly charged.

If all of the ions present have mobilities $k < k_c$, i.e., for points along the linear portion of[11] the *I-V* curve in Fig 15, the expression for the current reduces to

$$= \left(\frac{M_0}{k_c}\right)\int_0^{k_c} ekf(k)dk = \left(\frac{VC}{\varepsilon_0}\right); \tag{11}$$

This expression relates the conductivity of the air drawn through the Gerdien tube and a set of physical parameters that can be determined. Note that the result is independent of the volumetric air flow through the device. For the situation where some of the ions have mobilities $k > k_c$, the response is no longer proportional to conductivity, and the *I-V* characteristic is nonlinear. In terms of Eq 10, the integral from k_c to ∞ begins to contribute.

If all the ions are being collected, the curve saturates as shown in Fig 15; all the ions satisfy the condition k k_c, and the first integral in Eq 10 vanishes. Then

$$' = M_0 eN = M_0\rho \tag{12}$$

where

N = the total number of ions entering the Gerdien tube

In this mode of operation, the device is said to function as an ion counter.[12]

[11] See [32].

Because of the large mobility differences between small ions and charged particles, the *I-V* curve of an ion counter will display a plateau while all the small ions are being collected, even in the presence of charged particulates. This is technically not a "saturated" condition since, as the polarizing voltage is increased, a larger fraction of the less mobile particles will be collected. However, small ion densities are determined by operating the ion counter in this saturated condition (see Section 9). In practice, when conductivity measurements are performed, Gerdien tubes are operated with high flow rates and low polarizing potentials to assure that the device is operating on the linear part of the *I-V* curve. It is important that the proper operating conditions be established by determination of the *I-V* characteristic for the Gerdien tube being used. Although the conductivity measurement is one associated with small ions, if the air is heavily polluted the small-ion density may be substantially reduced and in fact represent only a small fraction of the ion population. If such conditions exist, an interpretation of the conductivity as being representative of the small-ion concentration may not be warranted.

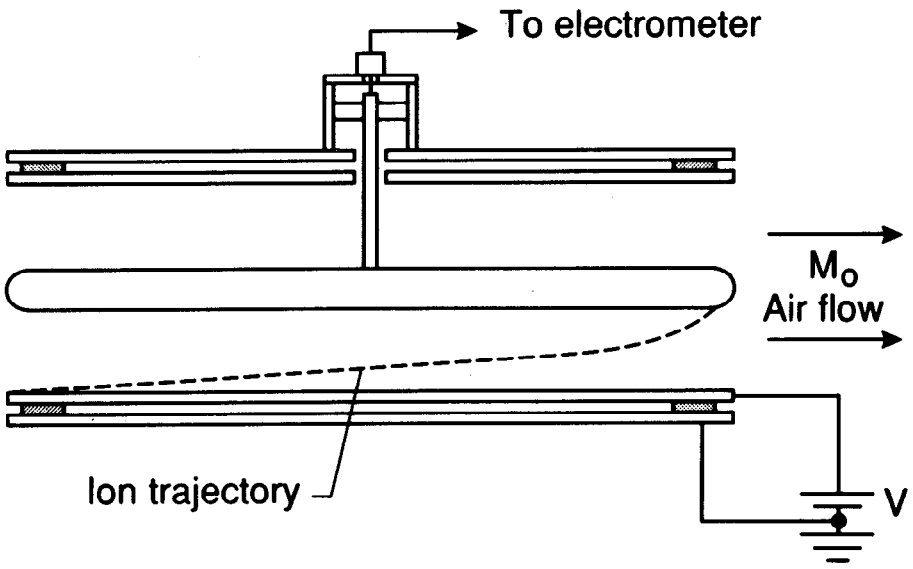

NOTE—The outer grounded cylinder is used to limit the extent of fringing fields (edge effect).

Figure 14 — Schematic View of a Gerdien Tube

[12]See [12], p. 196.

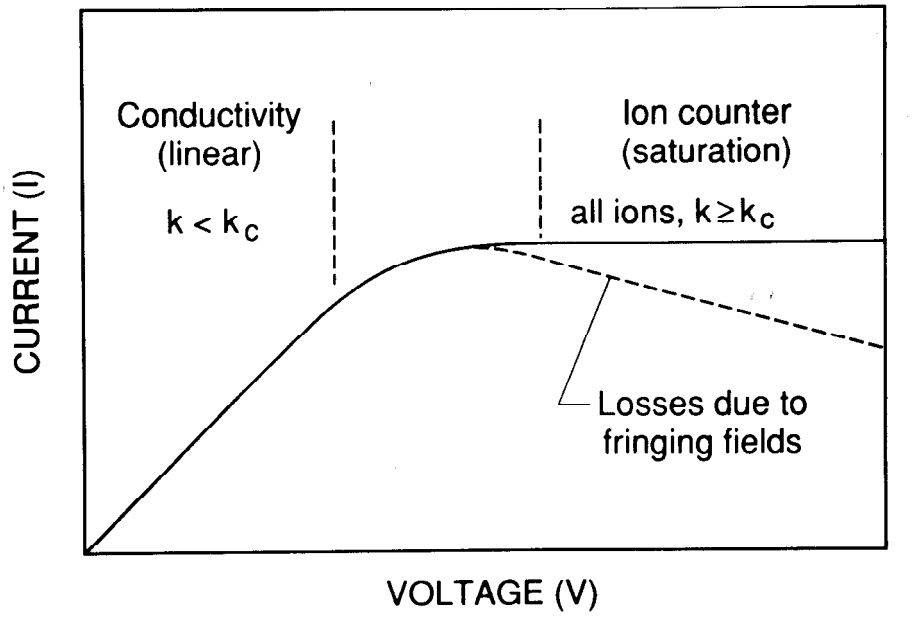

NOTE—Losses due to fringing-field effects are shown with a dashed line.

Figure 15 — Features of the I-V Curve for a Gerdien Tube for the Operating Range From Conductivity Measurements to Ion Counting

8.2 Calibration of Instrumentation.

To date, no experimental calibration of Gerdien tubes has been reported in the literature. This is due in part to the difficulty in establishing experimentally an ion source with a known mobility distribution, $f(k)$. In principle, the characteristics of these instruments are based on calculable or measurable quantities (i.e., V, C, I), but because of the number of potential sources of systematic errors, a means of calibration would be desirable.

One practical problem is the determination of the effective capacitance appearing in Eq 11, which is that associated with the active ion-collecting region of the Gerdien tube. A method for making this measurement is discussed in [63].[13]

8.3 Measurements.

As previously noted, conductivity measurements are not usually made near dc power lines. To date, only one account of conductivity measurements in the vicinity of a dc power line has been reported [28]. Reports of terrestrial conductivity measurements are given by Kraakevik [47], Higazi and Chalmers [29], and in references cited by Chalmers.[14]

[13]The method described in this reference is not strictly correct since it ignores the fact that the capacitance contributed by the support is a function of the total geometry and will be different with the central electrode in place. There is also an apparent typographical error in the equation $CR = \pi\lambda/4$. CR should be proportional to $1/\lambda$.

[14]See [12], p. 199 ff.

8.4 Sources of Measurement Error.

One source of systematic error associated with conductivity measurements made using the Gerdien tube results from the effects of fringing fields, which are sometimes called “edge effects.” These effects should be distinguished from those that are due to fields external to the instrument, which are discussed in 9.4. The polarizing potential, *V*, may be applied to the Gerdien tube in several ways, two of which are indicated in Fig 16. If the collector electrode is grounded (through the electrometer), as indicated in Fig 16(a), the polarizing potential on the outer electrode results in external fringing fields, which affect the measurement by retarding and causing the loss of incoming ions. The loss of ions is reflected in the current-voltage characteristic curve with the elimination of the plateau in Fig 15 (dashed line in Fig 15) as the polarizing voltage is increased. In an actual instrument design, this effect may be somewhat reduced by surrounding the outer electrode with a grounded cylinder that restricts the extent of the external field as indicated. When the polarizing potential is in series with the electrometer as shown in Fig 16(b), the external fringing field is reduced. In this case, the field can still “leak” to the outside and result in an increased number of ions that will be attracted to the collector rod. This condition can easily be detected by reducing the air flow through the tube to zero and noting the presence of current. For the configuration shown in Fig 16(b), there are severe restrictions on polarizing supply stability and leakage across insulators, since spurious signals are directly coupled to the electrometer. These problems can be minimized in a number of ways that are discussed in the literature [34], [45] and are summarized in an extensive treatise on ion counters [66].

Other sources of error are uncertainties in the measurement of *I* and *V*, and effects of an external dc electric field. For the charge densities encountered near dc power lines, the effects of Coulomb repulsion can also influence the measurement process. Several of the above error sources are considered further when monopolar charge-density measurements are discussed in 9.4.

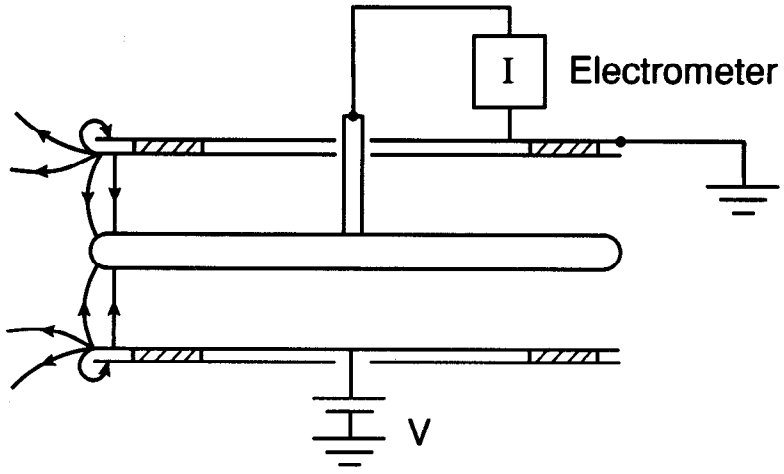

Figure 16a — A Gerdien Tube Polarizing Configuration Such That Ions Are Deflected at the Inlet

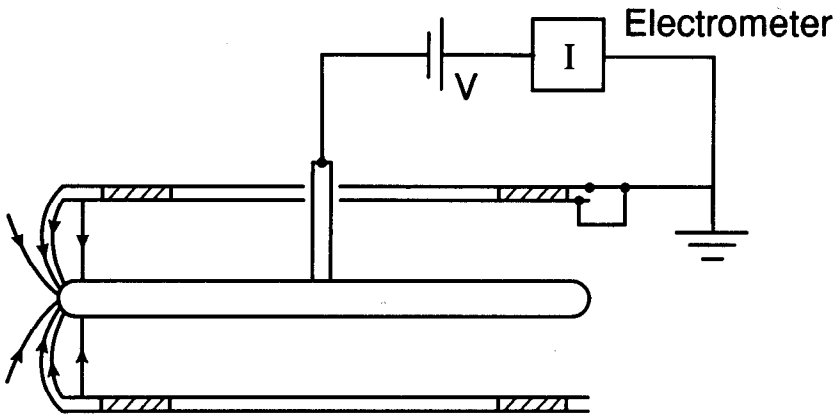

Figure 16b — Arrangement Where Fringing Fields Attract Ions to the Collector From Outside the Device

9. Monopolar Charge-Density Measurements

9.1 Instrumentation and Principle of Operation.

As indicated in Section 8, the aspirator-type instrumentation used for conductivity measurements can also be used for determining monopolar charge densities, provided it is

operated in the saturated current region (i.e., plateau region in Fig 15). In this mode of operation, the instrumentation has historically been referred to as an ion counter, although ions are not actually counted. From Eq 12, the charge density for ions with mobility greater than the critical mobility (Eq 10) is given by

$$\rho = \frac{I}{M_0} \tag{13}$$

where

I = the ion current
M_0 = the laminar volumetric flow rate through the ion counter

It is common practice to assume that all the ions collected are singly charged and to convert the measured charge density to an equivalent number of charges per unit volume [12]. Commercial instruments are frequently configured with voltages that can be selected to allow operation with different critical mobilities. In addition to cylindrical geometries (Fig 14), ion counters with parallel-plate geometries as shown in Fig 17 have been used for charge-density measurements [45]. Alternate plates are connected, and the groups of plates are connected to a polarizing potential and electrometer respectively. Ion counters can be operated in the ground plane by mounting the instrumentation vertically in a cavity below the ground plane, with the aperture flush with the ground plane. Sump pumps have been used to prevent flooding in the cavity when ion counters have been used in this configuration during long-term outdoor measurements [16].

Yet another method for determining monopolar charge density in the ground plane is to measure simultaneously the current density, J, and the electric-field strength, E, at ground level and use Eq 1 to calculate ρ, assuming a value for the average mobility, K, and that the air velocity is negligible [9], [11], [20]. While

relying solely on this approach for determining mobility is questionable because of the uncertainty associated with assuming the value of ion mobility, it can serve as a check of charge-density measurements obtained with an ion counter. Further discussion of this method is provided in the references cited above.

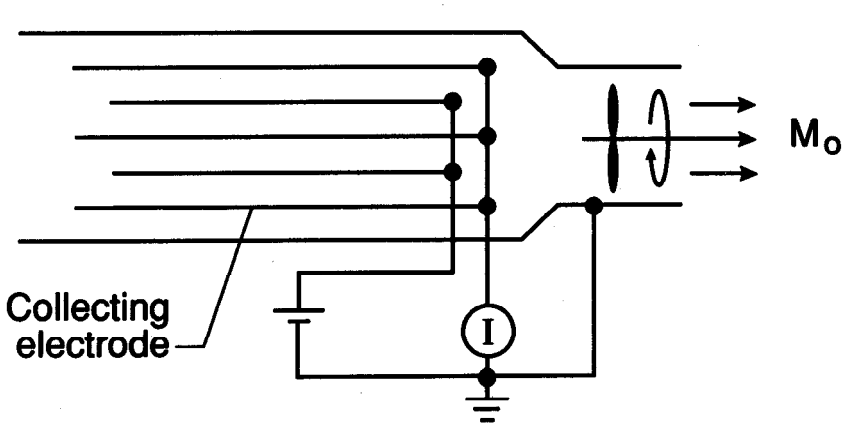

NOTE— The volume between the outer collector plate and the counter enclosure is inactive (no polarizing potential).

Figure 17 — Parallel-Plate Ion Counter

9.2 Calibration of Instrumentation.

An apparatus that produces a known charge density in the presence of dc electric fields, comparable to those near dc power lines, is required for experimental calibration of aspirator-type ion counters. The parallel-plate apparatus shown in Fig 7 is suitable for calibrating ion counters in the ground plane [57], [58]. To establish its suitability, it is necessary to demonstrate that

1) The unperturbed charge density profile, $\rho(z)$, between the parallel plates can be calculated, and
2) Significant perturbations of $\rho(z)$ due to the aperture of the ion counter in the ground plane and air flow through the aperture do not extend to the top plate of the parallel plates.

The influences of the dc electric field, air motion from the ion counter, Coulomb repulsion, and diffusion on the transport of ions into the ion counter must also be characterized to determine their effects on instrument calibration and measurements (see 9.4). A known charge density with an uncertainty of ±9% can be produced for calibration purposes using the parallel-plate apparatus in Fig 7. Fig 18 shows a comparison of calculated charge density and measured values using a parallel-plate ion counter—as a function of average air velocity through the ion counter. The calibration was performed with the ion counter aperture flush with the ground plane [58].

As suggested by the above remarks, calibration of aspirator-type ion counters is a complicated procedure. In addition, the validity of a calibration is limited to the charge density used at the time of the calibration because of duct losses due to Coulomb repulsion when large charge densities exist. Details of the calibration apparatus and procedures are given in [57] and [58]. Experimental calibration of ion counters that are used above the ground plane has not been reported. However, for certain conditions (see 9.4.3), calibration in the ground plane may be adequate for above-ground charge-density measurements.

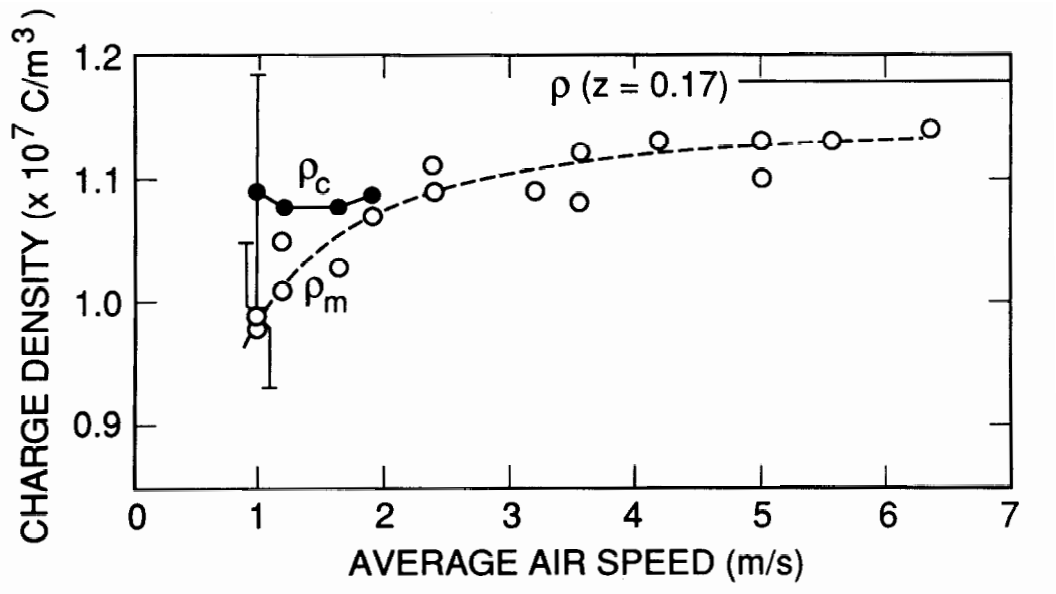

NOTE—Calculated values of the charge density, ρ_c, are shown for air speeds less than 2 m/s. Typical error bars are indicated for the results near an air speed of 1 m/s.

Figure 18 — Positive Charge-Density Measurements, ρ_m, as a Function of Average Air Velocity in the Plane of Aperture

9.3 Measurements

9.3.1 Power-Line Charge-Density Measurements.

Much of the discussion regarding power-line electric-field strength measurements in 6.3.1 applies to monopolar charge-density measurements, and the reader is encouraged to review the earlier section. Briefly:

1) The data can be obtained over an extended period to determine the range of charge-density values for specific weather conditions.
2) An automated data acquisition and storage system is used for monitoring signals from the ion counter and from sensors indicating weather conditions.
3) The measurements represent charge-density values near ground level.
4) The measurement techniques are applicable to areas outside a converter station building where significant levels of space charge may exist.

Ideally, lateral profile measurements of the charge density are desirable, but the cost of the instrumentation may restrict the measurements to only a few locations. As noted for the electric-field and current-density measurements, short-term measurements with perhaps less automated, portable instrumentation, lasting less than a week, may be satisfactory in cases where a more comprehensive data base is not required.

There are few accounts of monopolar charge-density measurements performed with ion counters in the vicinity of dc power lines. The first report appears to be that of Bracken and Furumasu [10] for measurements in the ground plane beneath a high-voltage test line at The Dalles in Oregon. The measurement locations were approximately ±8 m with respect to the center line.

Ground plane monopolar charge-density measurements have also been conducted at the Bonneville Power Administration Grizzly Mountain test site [16]. The measurement locations were ±7.9 m and ±22.9 m from the center of the transmission line at midspan.

While apparently no measurements of monopolar charge density have been made above the ground plane in the vicinity of power lines, measurements of terrestrial charge densities above the ground plane are extensively reported in the technical literature.[15]

9.3.2 Indoor Charge-Density Measurements.

Measurements of monopolar charge densities have been reported for indoor settings as part of studies dealing with ion-counter calibration and measurements [57], [58], indoor air quality [48], and small animal bioeffects [14], [15]. The references cited consider measurements in and above the ground plane. As for indoor electric-field-strength measurements (see 6.3.2) and current-density measurements (see 7.3.2), short-term measurements of the charge density are expected to reflect the nominal long-term density values both in the absence of nearby surfaces that could become charged unpredictably, and in the absence of changes in the source of ions. Significant changes in air composition are also assumed to be unlikely.

9.4 Sources of Measurement Error.

Ion-counter measurements can be subject to many sources of errors that, for purposes of discussion, may be divided into those associated with the interior of the ion counter and those external to the ion counter. The sometimes severe environmental effects that can be encountered during long-term outdoor measurements have previously been noted (see 6.4 and 7.4) and are discussed in [16]. Parameters external to the ion counter that can affect measurements of charge density are discussed first. Parameters that can influence the internal operation of an ion counter are then considered, followed by a discussion of above-ground-plane measurements. Only a brief description of the error sources are given with references cited to provide additional details. A comprehensive account of factors that influence ion-counter operation are provided in [34] and [66]. Maintenance procedures and in-the-field performance tests for ion counters used for long-term, unattended outdoor measurements are discussed in [16].

9.4.1 External Parameters Affecting Ion-Counter Operation.

The derivation of Eq 13, which is used to determine ρ, assumes that the electric field at the entrance of the ion counter is zero, the charge density being sampled is uniform, and the rate of laminar air flow through the ion counter, M_0, is known [66]. In the vicinity of high-voltage dc transmission lines, a significant electric field exists, the charge density distribution may not be well known, and the presence of wind can affect air flow through the ion counter. The effects of these factors are considered below.

9.4.1.1 External Electric Field.

Fig 19 shows approximate ion trajectory calculations for positive ions approaching the aperture of an ion counter that is mounted flush with the ground plane with and without the existence of an electric field [57], [58]. The dashed lines show ion trajectories with no external electric field and for a time-of-flight to the aperture of 50 ms. The air speed in the plane of the aperture is assumed to be uniform and equal to 1 m/s. Introduction of a 15 kV/m electric field modifies the trajectories for the same time-of-flight to the solid lines. The volume of ions that reaches the aperture of the ion counter with the presence of the electric field is significantly larger than without the field. Because the validity of Eq 13 rests on the assumption that ions are transported into the ion counter only by the air that flows through the ion counter, the extra ions can be regarded as a source of measurement error. However, theoretical [64][16] and experimental results [57], [58] indicate that the extra ions resulting from the external electric field will not reach the collecting electrodes, provided that the collecting electrodes are adequately shielded.

---

[15]See [12] and references cited therein, p. 94 ff.

[16]Swann's theory does not consider large ion densities for which there is significant Coulomb repulsion between the ions. However, the study described in [57] and [58] suggests, within experimental uncertainty, that the theory is valid even when Coulomb repulsion is significant.

This can be accomplished by designing the ion counter with a sufficiently long duct in front of the collecting electrode (see also 9.4.2 for Coulomb losses). Adequate electric-field shielding exists if there is no significant ion current to the collecting electrode when M_0 is made equal to zero.

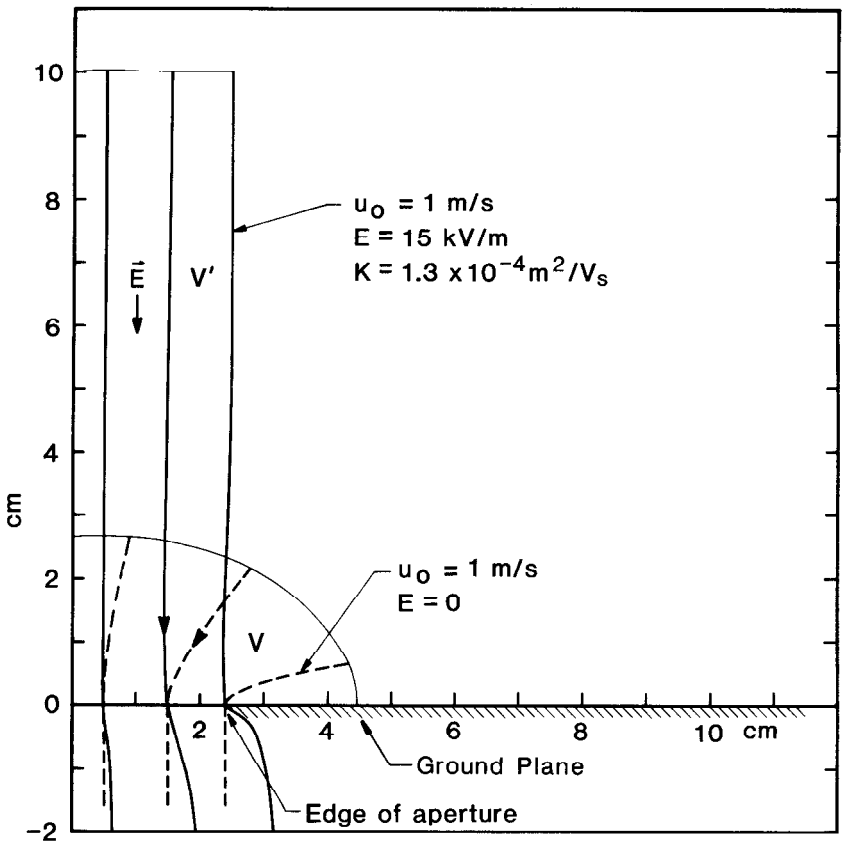

NOTE—The solid curves show the influence of a 15 kV/m electric field. Dashed curves are for no electric field. The time-of-flight for all trajectories is 50 ms. The volume occupied by the ions that enter the aperture when $E \neq 0$, V', exceeds the volume of air, V, that enters in the same time

Figure 19 — Ion Trajectories for Air Speed in the Plane of Aperture of 1 m/s.

9.4.1.2 Nonuniform Charge Density.

Eq 13 assumes that the charge density that is sampled by the ion counter is uniform. This may not be well approximated in the vicinity of a dc transmission line or in laboratory apparatus designed to simulate the transmission-line environment. The ion-counter measurement represents some average value and in general will not equal the charge density precisely at the ground plane [57] [58].

9.4.1.3 Wind.

Measurement of the volumetric flow rate is straightforward if a suitable flow meter is used, but this is usually not done in commercial instruments because of the cost of the flow meter. For these devices, the flow rate is determined by the manufacturer and is included in the instrument calibration. If the ion counter is operated in a situation where there are external winds, then the air flow through the instrument can be affected, and the stated instrument calibration may become invalid. Simultaneous measurements of wind as well as volumetric flow rate and ion current in an ion counter operating near dc power lines would be desirable to determine the degree of measurement perturbation resulting from wind action.

9.4.2 Parameters Affecting Internal Operation of the Ion Counter

9.4.2.1 Fringing Electric Field.

The loss of ions due to fringing fields as outlined in 8.4 during the discussion of conductivity measurements can also occur for a cylindrical ion counter and is not discussed further here. The parallel-plate ion counter can exhibit similar losses if the electrode geometry is not properly designed. The plates with the polarizing voltage shall be sufficiently recessed behind the collecting plates to avoid significant loss of ions. Measurements that show the loss of ions because of fringing-field effects are presented in Fig 20 [57]. As the polarizing plates are moved from positions in front of the collecting plates to recessed locations, the loss of ions decreases to a negligible level for increasing polarizing voltage. The flow rate and charge density were held constant during these measurements. A useful empirical guide is that the polarizing plates should be recessed two plate spacings behind the front of the collection plates. The presence of fringing-field effects is best determined by measuring the *I-V* characteristic curve of the ion counter and observing whether a droop occurs in the "plateau" (Fig 15).

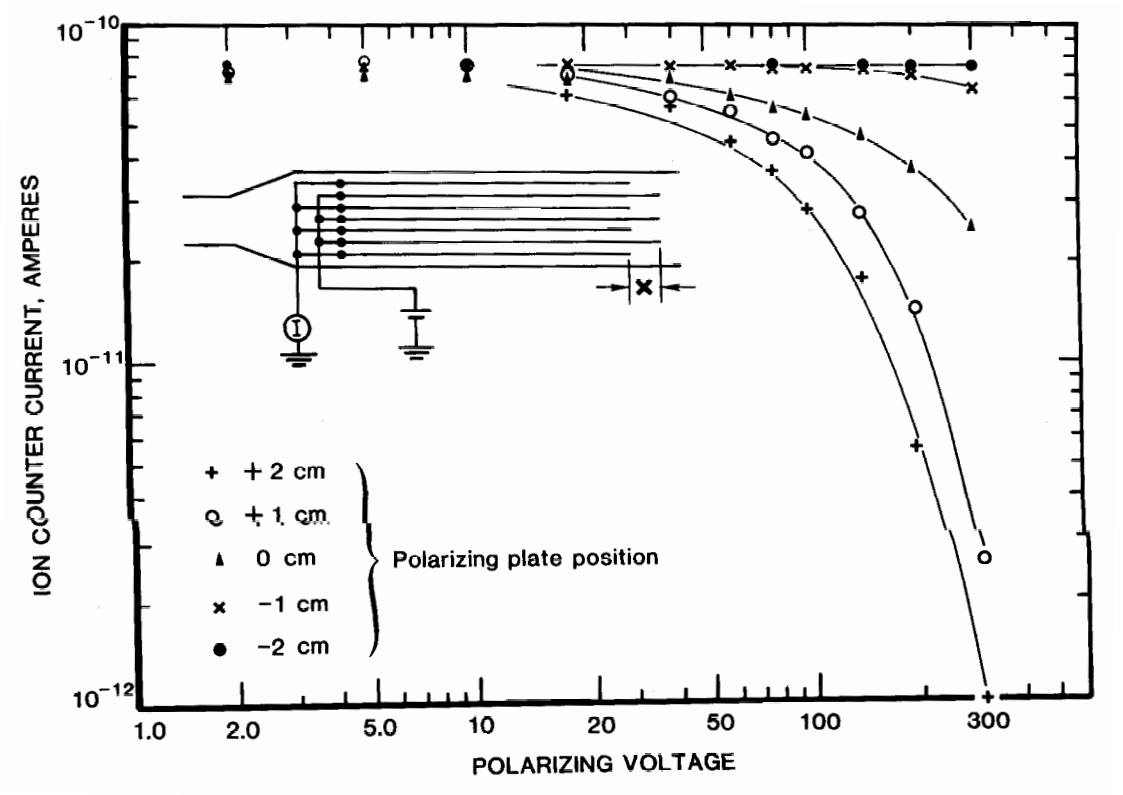

NOTE—The displacement between the leading edges of the collection and the polarizing plates is *x*. Positive values of *x* correspond to a situation where the polarizing plates protrude in front on the collector plates. For $x = 0$, the leading edges were flush. Because the ion density is independent of the polarizing voltage over the range plotted, the ion-counter current should be constant. The spacing of the parallel plates is near 1 cm and the air speed, averaged over the area of the ion-counter aperture, is near 42 cm/s.

Figure 20 — Ion-Counter Output Current as a Function of Polarizing Voltage for Different Plate Configurations

9.4.2.2 Coulomb Repulsion and Diffusion.

As noted in 9.4.1.1, the measurement error due to an external electric field can be made negligible by adequately shielding the ion-counter

collecting plates with a length of duct. This procedure, however, introduces two mechanisms for ion loss, namely by Coulomb repulsion due to the large charge densities near dc transmission lines, and diffusion. The effects of turbulence may also lead to ion losses for a sufficiently high Reynolds number. An approximate expression for the charge density (when Coulomb repulsion is the only mechanism for loss), $\rho(L)$, after a circular cylinder of charge has traversed a distance L in a cylindrical duct is given by [57], [58]

$$\rho(L) = \frac{\rho_0 R^2}{(R+s)^2} \tag{14}$$

where

$$s = \frac{K\rho_0 RL}{2\varepsilon_0 u}$$

In Eq 14,

ρ_0 = the initial charge density
R = the radius of the duct
K = the average mobility
u = the air velocity

A more exact expression for ρ that is independent of geometry is [41]

$$\rho = \frac{\rho_0}{\left[1 + \frac{\rho_o K\tau}{\varepsilon_0}\right]} \tag{15}$$

where

τ = the time-of-flight between the initial and final points of observation

The radial displacement of ions due to diffusion for a cylindrical cloud of ions as it traverses a cylindrical duct also leads to ion losses. An expression for this radial displacement, s', is given by [57], [58]

$$s' = \left[\frac{4kTKL}{ue}\right]^{1/2} \tag{16}$$

where

k = the Boltzmann constant
T = the temperature in degrees K
e = the ionic charge

A further discussion of duct losses is given in [57] and [58]. Losses due to Coulomb repulsion and diffusion can be reduced by placing an aperture at the entrance of the duct that is smaller in area than the cross-sectional area of the duct. It is cautioned, however, that adding a duct and aperture to a commercial ion counter could affect the air flow (M_0) because of the increased load on the fan.

9.4.2.3 Other Parameters.

In addition to the fringing field, Coulomb repulsion, and diffusion effects described above, the internal operation of an ion counter can be affected by

1) Exposed insulating surfaces that can become charged and deflect ions
2) Vibrations of the ion-counter electrodes, which can produce microphonic signals that obscure the ion-current signal during measurement of low-charge densities [16]
3) Instabilities in the power supply providing the polarizing voltage, which capacitively couple to the electrometer circuit and perturb the ion-current measurement (batteries should be used when possible)
4) Air flow between the outside collecting plate and ion-counter enclosure (Fig 17), which leads to poorer collection efficiency of the ions
5) High relative humidity, which can cause leakage currents and affect the value of high resistances in the electrometer circuit [16]
6) Accuracy of the voltmeter and electrometer that are used to measure V and I
7) Coulomb repulsion between ions, which occurs between the electrodes of the ion counter
8) Turbulence of the air motion between the electrodes of the ion counter

Heaters have been used in ion counters to minimize moisture-related errors during long-term outdoor measurements [16].

9.4.3 Charge-Density Measurement Above the Ground Plane.

Ion counters are often operated above the ground plane for reasons of convenience. Fig 21 schematically shows ion counters in two orientations above the ground plane for measuring positive-charge densities in the presence of a uniform vertical electric field. The housing of the ion counter is shown electrically floating in Figs 21(a) and 21(d), referenced to ground potential in Figs 21(b) and 21(e), and biased to attract positive ions in Figs 21(c) and 21(f).

Measurements with the horizontal orientation are less affected by rain or snow, but some positive ions will fail to reach the aperture of the ion counter in Fig 21(a) because of the opposing electric field or, equivalently, because of the repulsion between the induced positive charges on the housing and the approaching ions [57], [64]. The problem is reduced in Fig 21(b) and eliminated with the attractive bias shown in Fig 21(c). With the vertical orientation, few if any positive ions approaching the aperture of the ion counter will be repelled by the induced charges on the housing in Figs 21(d) and 21(e), and no ions will be repelled with the attractive bias in Fig 21(f). Although the electric field can increase the number of ions reaching the aperture to a value in excess of that due to the aspirating action of the ion counter alone, the extra ions will not be measured provided there is adequate electric-field shielding of the collecting electrodes (see 9.4.1.1).

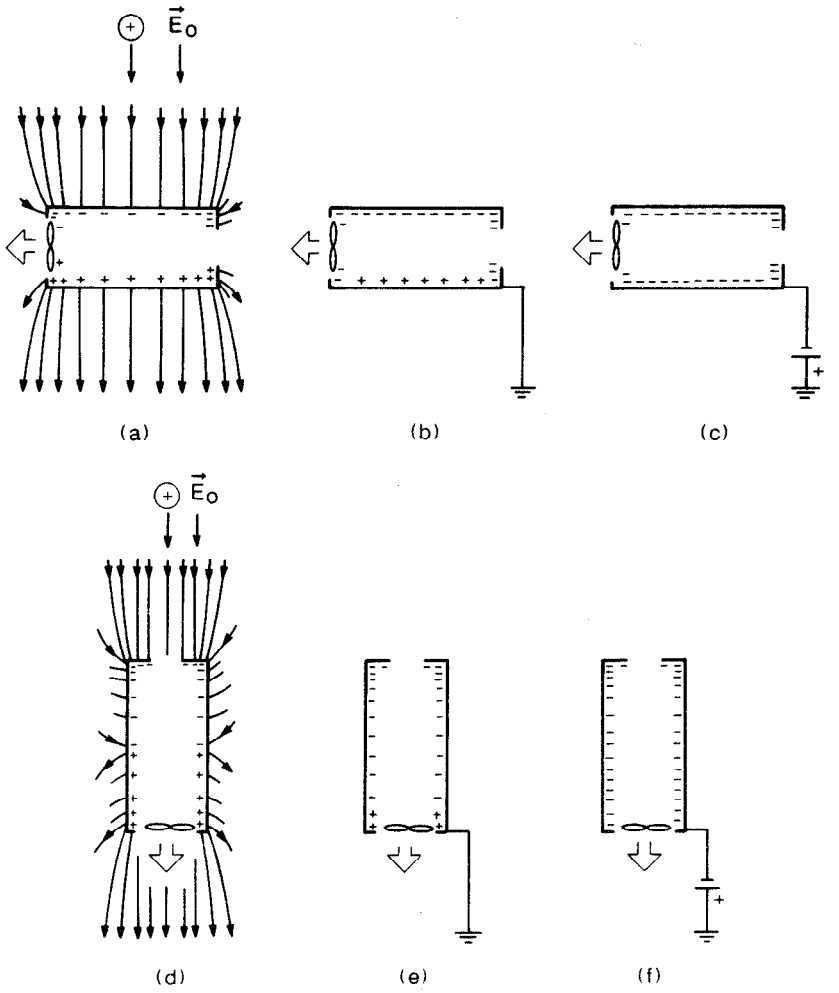

NOTE—Induced charges produced by a uniform vertical electric field, E_0, are shown when the ion-counter housing is at space potential in (a) and (d), referenced to ground in (b) and (e) (the number of positive charges depends on the difference in potential between the ion-counter housing and the ambient space potential), and biased to attract positive ions in (c) and (f).

Figure 21 — Schematic Views of the Ion Counter Above the Ground Plane in Vertical and Horizontal Orientations

10. Net Space-Charge-Density Measurements

10.1 Instrumentation and Principle of Operation.

Two types of instrumentation for measuring net space charge are considered in this guide, the Faraday cage and the filter [5], [67]. The use of ion counters to measure charge densities of each polarity (with uncertainties typically in excess of ±10%) and subtracting the measurement results to obtain the net space charge is not recommended because of the large errors that can occur when the densities of ions of each polarity are comparable. In this regard, it should be noted that it is possible to have nearly zero net space-charge density at a location, but very large positive- and negative-charge densities. Faraday cages can only be used in outdoor settings and have been employed for measuring net space charge near dc power lines and test lines [11], [16], [36]. Filters can be used for both indoor and outdoor applications.

10.1.1 Faraday Cage.

In the Faraday cage measurement approach, an enclosure made of coarse conducting mesh (the Faraday cage) is located in the region where the measurement is to be made; the mesh is held at ground potential. The construction of the cage should be such that

1) There is adequate electric-field shielding of the interior region
2) The loss of space charge to the mesh is negligible as air motion transports ions into the cages

Faraday cages have been constructed of wire mesh with approximately 1 cm spacing between adjacent wires [5], [11].

Assuming that the space charge enters and uniformly fills the cage, the electric potential at an interior point can be determined by solving Poisson's equation. For a rectangular parallelepiped enclosure, the solution of Poisson's equation is [5]

$$(x,y,z) = \left(\frac{64\rho_s}{\pi^5\varepsilon_0}\right) \times \sum_{\substack{ijk \\ odd}} \frac{\sin\left(\frac{\pi i x}{a}\right)\sin\left(\frac{\pi j y}{b}\right)\sin\left(\frac{\pi k z}{c}\right)}{ijk\left[\left(\frac{i}{a}\right)^2 + \left(\frac{j}{b}\right)^2 + \left(\frac{k}{c}\right)^2\right]} \tag{17}$$

where

ρ_s = the net space charge density in the cage
a,b,c = the dimensions of the cage as shown in Fig 22
$\in_0$ = the permittivity of free space

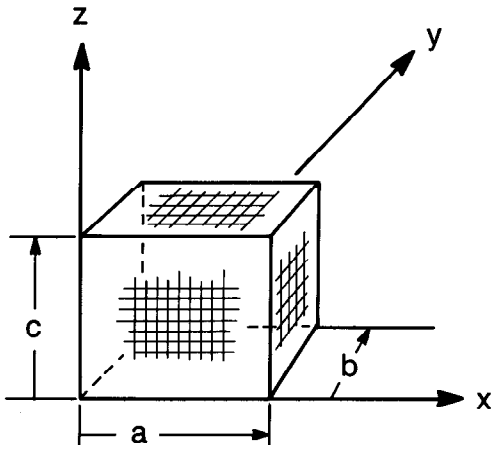

Figure 22 — Schematic View of a Parallelepiped Faraday Cage and Coordinate System for Eq 17

For a cubical enclosure of side dimension *L*, Eq 17 reduces to the result of Eq 18 at the center of the cube [52].

$$\phi = 6.32 \times 10^9 \rho_s L^2 \tag{18}$$

Thus, measurement of the potential at the center of the Faraday cage allows the determination of the net space charge. In Eq 18, ρ_s is in units of C/m^3 and *L* is in units of meters. From Eq 18, the potential at the center is equal to 10 V when *L* is equal to 1 m and the space charge is 1.6×10^{-9} C/m^3 (10^4 ions/cm^3). Eq 18 shows the more general result, that the sensitivity of the potential measurement can be increased by increasing the size of the Faraday cage.

An outline for solving Poisson's equation for cylindrical geometries is described in the literature [6]. The expression for potential at the center of a cylindrical Faraday cage, ϕ'_c, 1 m in height and 1 m in diameter, is given by [11]

$$\phi'_c = (9.28 \times 10^9)(0.611)\rho \quad (19)$$

The potential at the center of a Faraday cage can be measured using a radioactively equilibrated probe [36][17] and appropriate electronic circuitry. Fig 23, taken from reference [36], shows a schematic view of a space-potential probe circuit used for such measurements. The potential of the probe is measured using a high-impedance unity gain voltage follower. The large voltage swings, which can occur for measurements near dc power lines, is obtained by slaving a high-voltage amplifier to the high-impedance amplifier as shown in Fig 23. The high-impedance amplifier (voltage follower) and its battery power supply are electrically floated on the output of the slave high-voltage amplifier. Potentials between -150 V and +150 V can be measured with the circuit shown in Fig 23. The sensitivity and response time of the probe to fluctuations in the space charge are improved by symmetrically placing a weak radioactive source, such as polonium 210 (Po 210), on the tip of the probe. The radioactive source generates large numbers of ion pairs in the Faraday cage, but because equal numbers of ions of both polarities are produced, the net space charge is assumed to be unaffected.

It is possible to determine the electric-field strength at any point in the parallelepiped Faraday cage by taking the gradient of the potential (Eq 18). This operation can provide a relationship between the electric-field strength at the surface of the Faraday cage and the charge density within [5]. Thus, measurement of the electric-field strength at the surface of a Faraday cage also allows the determination of the space-charge density. For the cubical Faraday cage considered earlier, where L = 1 m and ρ_s = 1.6 x 10^{-9} C/m^3, the electric-field strength at the center of one of the faces is 50 V/m. However, measurements of such low electric fields are prone to error because of instabilities and drift in the instrumentation (see 6.4).

No systematic study has been performed to determine the minimum air velocity required for adequate ventilation of Faraday cages. Anderson [5] presents arguments that air velocities in excess of 1 m/s should be satisfactory to avoid ion losses by diffusion to the cage mesh as the ions enter the cage, assuming mesh openings of 1.35 x 10^{-4} m^2.

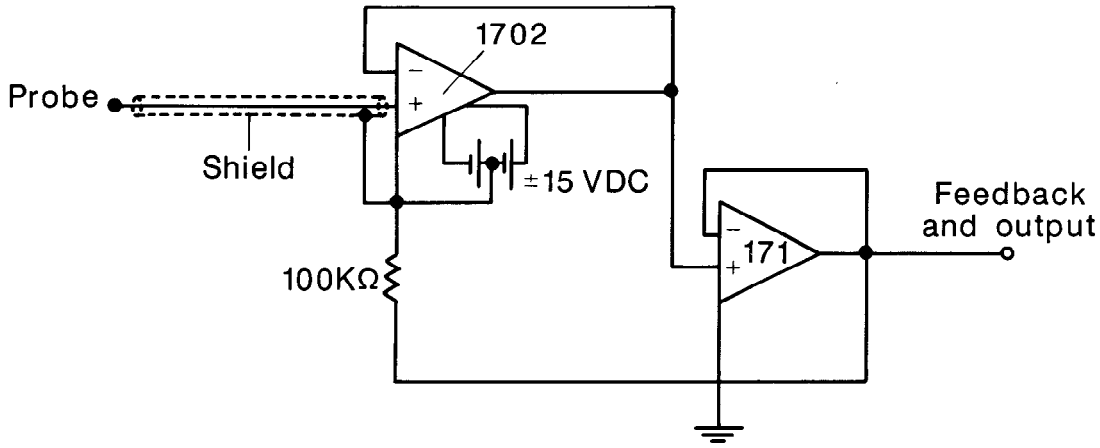

NOTE—A high-voltage operational amplifier (171) is “slaved” to the high-impedance battery operated amplifier (1702) to permit measurements of voltages from -150 V to 150 V.

Figure 23 — Diagram of the High-Impedance Voltage Follower Circuit Used to Measure the Potential at the Center of the Faraday Cage

[17]See [12], p. 128.

10.1.2 Filter.

A second method for measuring net space charge is known as the filtration method [67] and is illustrated in Fig 24. Here, an air sample is drawn into a metal enclosure with a filter through which all the air passes. The filter is electrically isolated from the enclosure and ground so that the current, I, resulting from the charge removed from the air stream by the filter, can be measured. From this current, the net space-charge density can be calculated from the expression

$$\rho_s = \frac{I}{M_0} \tag{20}$$

where

M_0 = the volumetric air flow through the filter

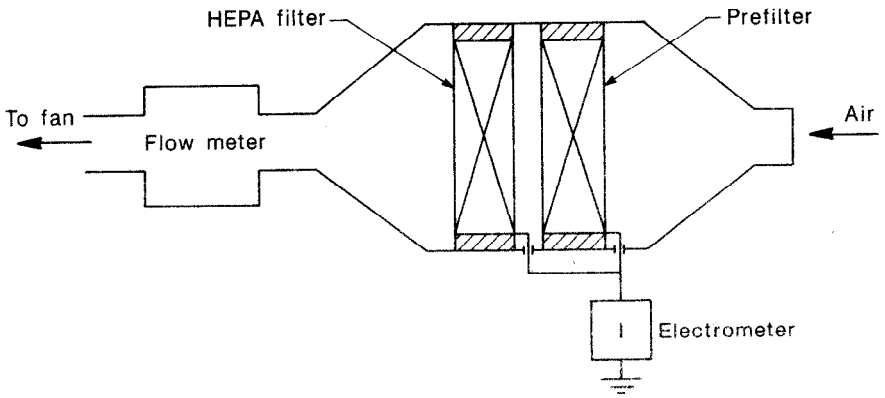

NOTE—Both prefilter and HEPA filters are isolated from ground and the filter housing.

Figure 24 — Schematic View of a Filter for Measuring the Net Space Charge

This method of measuring space charge assumes that the filter collects all of the charge in the air stream. High-efficiency air particulate (HEPA) filters are adequate for this application because tests with such filters indicate that the collection efficiency for small air ions can exceed 99.8% [7], [53]. HEPA filters also satisfy the requirement that the pressure drop across the filter be small enough to permit a high volumetric flow, which is necessary for developing a readily measurable rate of charge capture. Measurable currents of small air ions and collection efficiencies in excess of 99.9% have been reported for air speeds in excess of 1 m/s [53].

To prolong the life of the HEPA filter, it is common practice to employ a prefilter made of such materials as stainless-steel wool and glass fibers. Polytetrafluoroethylene (PTFE) has been used to provide electrical insulation between the filter element and outer casing because of its good insulating properties and negligible piezoelectric effect. To avoid the buildup of static charge on the PTFE due to frictional effects, the insulator should be shielded from the air moving through the filter enclosure [7].

10.2 Calibration of Faraday Cages and Filters.

Because sources of space charge with a known mix of positive and negative ions are not presently available, experimental calibrations of Faraday cages and filters cannot be performed. Space-charge density is determined using Eqs 18, 19, and 20, which represent idealizations of the actual measurement conditions. The parallel-plate apparatus described in 6.2.2, which can produce a known monopolar charge density, is not appropriate for calibrating filters because of error mechanisms that are a function of ion polarity in the presence of an electric field (see 10.4.2).

Instrumentation used for measuring the space potential in a Faraday cage (Eq 17) and the ion current and flow rate in a filter (Eq 20) should be calibrated when possible. The calibration of a space-potential probe for use in a Faraday cage is rather involved because of the difficulty in establishing a known space potential at a point in space in the presence of ions and a dc electric field. For example, the somewhat complicated parallel-plate apparatus described in 6.2.1 appears suitable for this application [57].

The electrometer used for measuring ion current intercepted by a filter can be calibrated using the current injection procedure described in 7.2. However, because of difficulties associated with calibrating flowmeters used for measuring volumetric flow rate (M_0 in Eq 20), in general it will be necessary to rely on the specifications provided by the manufacturer.

10.3 Measurements

10.3.1 Power-Line Space-Charge-Density Measurements.

While a large body of literature exists for outdoor ambient space-charge measurements, only a limited number of reports of measurements near power lines exist [11], [16], [36]. All of the measurements have been performed outside the right-of-way using Faraday cages. No use of filters has been reported.

The procedure for obtaining space-charge-density measurements near power lines parallels that for the other electrical parameters discussed in 6.3, 7.3, and 9.3. Because of the large variation in space charge due to factors such as rain, fog, fair weather seasonal effects, wind speed, and wind direction, an automated data acquisition system is used to monitor the various parameters if a comprehensive characterization of the net space charge environment is desired. Measurements are recorded as frequently as once per minute. From a large data base accumulated over a period of many weeks or months, values of space charge can be presented as functions of certain parameters that allow a clearer understanding of the measurements. For example, space-charge values are presented in Fig 25 as a function of distance from a monopolar dc test line for various wind speeds [11]. In Fig 25, it should be noted that only the data points at 70 m, 150 m, and 300 m are obtained using Faraday cages. The data points under the test line and at 20 m and 30 m are determined by measuring J and E simultaneously at ground level, assuming an average ion mobility and negligible air velocity, and using Eq 1. Each point represents an average determined by taking into account only fair-weather data for which the wind speed is as indicated in the figure and the wind direction is within ±20° of being perpendicular to the test line [11]. Such “filtering” of the measurement results is necessary to interpret the data properly. The cage measurements shown in Fig 25 were obtained with the Faraday cages elevated 3 m above the ground. Faraday cage measurements of net space charge are normally performed outside the power line right-of-way to avoid significant errors due to the effects of the electric field (see 10.4.1). As noted in discussions for measurement of the other electrical parameters, short-term measurements with perhaps less automated, portable instrumentation, lasting less than a week, can also be performed in cases where a more comprehensive data base is not required.

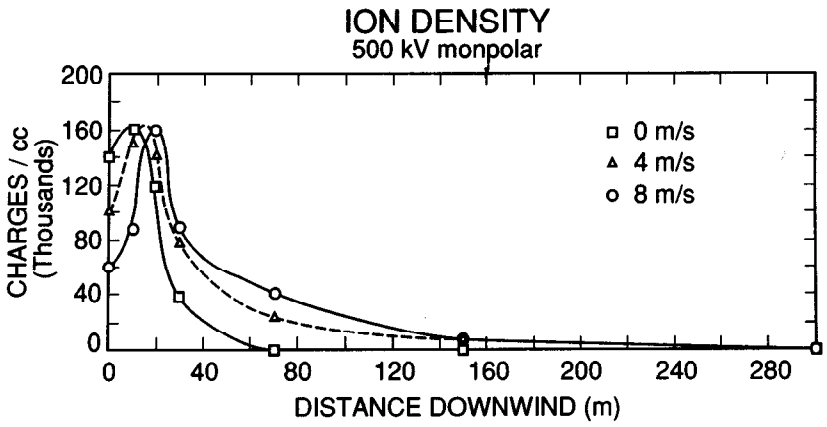

NOTE—The conductor is located at +10 m. As the wind increases from calm conditions to 8 m/s, the peak of the small air ion density shifts from the conductor to a position about 10 m downwind from the conductor.

Figure 25 — Small Air Ion Density Plotted Versus Distance for Wind Speeds of 0 m/s, 4 m/s, and 8 m/s

10.3.2 Indoor Space-Charge-Density Measurements.

Filters can be used for indoor measurements of space-charge density because they do not rely on wind motion for ion transport into the instrumentation. Indoor space-charge-density measurements with filters have been reported in connection with studies of the efficiency of HEPA filters [7], [53], the efficiency of electrostatic precipitators for cleaning air [69], and the soiling ability of airborne particulates [70]. While these studies do not relate to electric-power transmission or distribution, the reader may wish to consult these references for further details of the experimental arrangements.

10.4 Sources of Measurement Error

10.4.1 Faraday Cages.

Use of Eqs 18 and 19 assumes a uniform space-charge density outside the Faraday cage that is transported undisturbed into the cage by wind motion. Near dc power lines there are significant electric fields, and the ions are transported into the cage by the combined action of the electric field and air motion (wind), a process similar to that for ion counters (see Section 9). Unlike ion-counter measurements, the determination of space charge requires taking into account ions of both polarities. Therefore, it is important to note that the influence of the electric field is to favor ions of one polarity in their movement toward the cage and hinder ions of the opposite polarity. Modeling the transport of ions into the Faraday cage is difficult for cubical and cylindrical geometries. However, estimates of the number of ions failing to enter a Faraday cage because of electric-field effects can be made for a grounded hemispheric cage in a uniform field, using an expression developed by Swann as part of a study of ion-counter operation [64]. A hemispheric cage at ground potential, resting on a ground plane in a uniform positive electric field, E_0, is shown in Fig 26. For this situation, the electric field will prevent some negative ions from entering the cage. It is assumed that the negative charge densities outside and inside the cage near a point P are uniform and are given by ρ_0 and ρ_i respectively. For a wind parallel to the earth's surface, the fractional change in negative ion density is given by [64]

$$\frac{\rho_0 - \rho_i)}{\rho_0} = \frac{3E_0 k \tan\epsilon}{v_a} \tag{21}$$

where

v_a = the wind speed
k = the ion mobility
θ = the angle between the radius to point *P*and the earth (Fig 26)

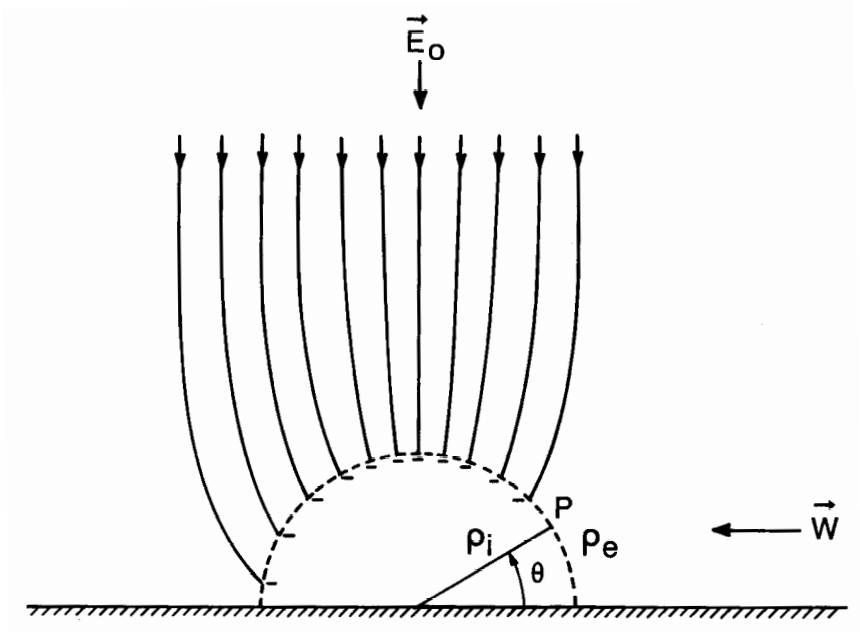

NOTE—The electric field reduces the number of negative ions that can reach and enter the hemisphere.

Figure 26 — Schematic View of a Hemispheric Cage Resting on the Ground Plane in a Uniform Vertical Electric Field, E_0

It is interesting to calculate the value of E_0 that prevents all negative ions from entering the cage at a given point, i.e., when the left-hand side of Eq 21 is unity. For v_a = 2 m/s, $k = 1.7 \times 10^{-4}$ m^2/Vs, and θ = 30° (halfway up the "side" of the hemisphere), the value of E_0 is 6.8 kV/m. As the size of the ion increases, the associated mobility will decrease, and the effect of the electric field will, according to Eq 21, diminish. For example, the mobility of a charged aerosol can be as small as 10^{-8} m^2/Vs [3], and the influence of electric fields on ion transport near power lines is then negligible.

A numerical calculation of the field at the surface of a cylindrical cage such as that described in 10.1.1 shows that the field-strength values along the side of the cylinder, which would oppose the entry of negative ions, are smaller than the hemispheric case for nearly 70% of the cylinder height, but larger than the hemispheric case closer to the top of the cylinder. Thus, the hemispheric model can be useful for making rough estimates of the influence of the electric field on the performance of a cylindrical Faraday cage, assuming some value for mobility. In any event, significant numbers of ions of one polarity could fail to enter the Faraday cage in the presence of electric fields comparable to those near dc power lines.

Because of the positive electric field in the above example, the number of positive ions arriving at the cage is increased. However, as for ion-counter measurements (see 9.4.1.1), theoretical arguments [64] supported by experimental studies [57], [58] indicate that the extra ions due to the electric field will not enter the interior of the Faraday cage provided that the electric-field shielding by the mesh is adequate.

Therefore, in the presence of dc electric fields, it is possible to erroneously measure excessively large values of net space charge. It should also be noted that if the space charge is predominantly monopolar ions and the

electric field is such that it enhances the number of ions arriving at the Faraday cage, the measurement error due to the electric field may be negligible if the shielding is adequate.

As noted in 10.1.1, the Faraday cage screening shall be sufficiently fine to exclude external electric fields but coarse enough to prevent significant diffusion to the screen. Anderson [5] reports that a cubical Faraday cage of 2.37 m side dimension, constructed of half-inch galvanized hardware cloth, with an additional layer of copper fly-screen across the top, is adequate for shielding the earth's electric field. A rough but conservative model calculation also indicates that the loss of ions by diffusion to the cage mesh is less than 3% for a wind speed of 1 m/s [5].

Establishing the adequacy of the electric shielding does not appear to be a straightforward process. Anderson describes a procedure outdoors lasting several days, during which the absence of correlations is sought between electric-field measurements of the Faraday cage interior and the ambient terrestrial electric field outside the cage [5]. Presumably, the same approach could be used more efficiently in a laboratory setting, during which a dc electric field external to the Faraday cage could be varied in a known fashion.

In addition to the uncertainty associated with the calibration of the space-potential probe (see 10.2), it is expected that the space-potential probe and probe shielding (Fig 23) will also perturb the space potential that is being measured. Because of the complex geometry of the equipotential surfaces inside the Faraday cage, this perturbation cannot be minimized by introducing the space-potential probe along an equipotential surface as is possible for a parallel-plate geometry [56]. The magnitude of the error related to this perturbation is, in general, unknown.

As noted in 10.1.1, the potential at the center of a Faraday cage can be measured with a space-potential probe with a radioactive source attached to the probe for improved coupling to the ambient space potential. Theoretical arguments indicate that the space-potential measurement can be perturbed if the geometry of the radioactivity is asymmetric and that the perturbation also depends on wind velocity [31].[18] Tests with an asymmetrically mounted radioactive source have shown that the space-potential measurement varies as a function of wind velocity as well as by orientation of the source with respect to the wind direction [60].

10.4.2 Filters.

As for the case of measurements with Faraday cages (see 10.4.1), the presence of an electric field can influence measurements of space charge using a filter. Eq 20, which is used to measure net space charge, is derived assuming that the ions are transported into the filter by the air drawn through the filter. However, ions are transported to the filter aperture under the combined effects of air motion and electric field. The electric field can discriminate against the arrival of ions of one polarity and favor ions of the opposite polarity.

Use can be made of Fig 21 for identifying an optimum arrangement for filter measurements above the ground plane. Taking the ion-counter housing in Fig 21 to be that of a filter, it is apparent that the optimum configuration for net space-charge-density measurements (but not monopolar charge-density measurements) is the horizontal orientation with the housing electrically floating at space potential, i.e., Fig 21(a). Only for this configuration will ions of both polarities be discriminated against by the induced charges near the aperture. If the positive and negative ions have comparable mobilities, the percentage of positive and negative ions repulsed by the induced charges will also be comparable. However, even with equal discrimination against ions of both polarities, the net space-charge measurement can be adversely affected unless the net space charge is zero.

Measurements of space charge using a filter above the ground plane, with the filter housing at space potential, are reported by Crozier [19]. However, details of the experimental arrangement are not provided. Extra ions that arrive at the aperture because of the electric field (see 9.4.1.1) will not be measured if the filter ele-

[18] See [12], p. 128.

ment is adequately shielded by the filter housing. The electrical shielding can be checked by noting whether there is any ion current to the filter when the flow rate, M_0, is zero.

Arguments similar to those made above will also show that measurements of space charge at ground level, with the filter aperture flush with the ground plane, may also be adversely affected by an electric field.

Some sources of error during monopolar charge-density measurements are common to filter measurements. The effects of wind and wind gusts (see 9.4.1.3), ion losses in the filter housing due to Coulomb repulsion and diffusion (see 9.4.2.2), exposed insulating surfaces that become charged, and air turbulence may have an effect on measurement accuracy. Current leakage across insulating surfaces may occur during humid weather conditions, affecting the measurement of I in Eq 20. Heater elements have been used in filters to keep insulating surfaces dry [7]. Because the filter element may become clogged with use, the volumetric air flow rate, M_0, should be monitored. As noted earlier, prefilters should be used to increase the life of the HEPA filter.

While the electrically isolated configuration in Fig 21(a) has been described as the optimum one for net space-charge-density measurements with a filter, it is noted that the housing of the filter can become charged because of the electric field and space charge. The charges on the housing can then repel ions of like polarity and perturb the net space-charge-density measurement. This problem may be overcome by maintaining the housing at space potential by means of a servo circuit that measures the space potential with respect to ground) at the height of the filter and applies a voltage to the housing equal to that of the potential difference [25].

Finally, it is noted that the influence of the electric field on measurements with the filter decreases as the ion size increases and the associated mobility decreases. The transport of ions into the filter is then determined more by air motion due to the aspirating action of the filter and the ambient wind.